

## 7.2 Artículos

### Artículo 1

Título: Using mobile device's sensors to identify fishing activity

Autores: **M. M. Galotto-Tebar**, A. Pomares-Padilla, I. A. Czerwinski y  
J. C. Gutiérrez-Estrada.

Revista: Journal of Marine Science and Technology

Volumen, número, páginas: 25(3), 978-989

Año: 2019

DOI: 10.1007/s00773-019-00694-5

Índice de impacto JCR (2019): 1.446

Recibido el 8 de febrero de 2019; aceptado el 12 de noviembre de 2019; publicado el 20 de noviembre de 2019; fecha de edición septiembre 2020.

Categoría de JCR	Clasificación en la categoría	Cuartil en la categoría
<b>Engineering, Marine</b>	<b>7 de 14</b>	<b>Q2</b>

### Artículo 2

Título: Is the vessel fishing? Discrimination of fishing activity with low-cost intelligent mobile devices through traditional and heuristic approaches

Autores: **M. M. Galotto-Tebar**, A. Pomares-Padilla, I. A. Czerwinski y  
J. C. Gutiérrez-Estrada.

Revista: Expert Systems With Applications

Índice de impacto JCR (2020): 6.954

Enviado el 12 de noviembre de 2020; primera revisión enviada el 26 de marzo de 2021; segunda revisión enviada el 20 de septiembre de 2021.

Categoría de JCR	Clasificación en la categoría	Cuartil en la categoría
<b>Engineering, Electrical and Electronic</b>	<b>24 de 273</b>	<b>Q1-D1</b>

# *Using mobile device's sensors to identify fishing activity*

**M. M. Galotto-Tebar, A. Pomares-Padilla, I. A. Czerwinski & J. C. Gutiérrez-Estrada**

**Journal of Marine Science and Technology**

Official Journal of the Japan Society of Naval Architects and Ocean Engineers (JASNAOE)

ISSN 0948-4280

J Mar Sci Technol  
DOI 10.1007/s00773-019-00694-5





# Using mobile device's sensors to identify fishing activity

M. M. Galotto-Tebar<sup>1</sup> · A. Pomares-Padilla<sup>1</sup> · I. A. Czerwinski<sup>2</sup> · J. C. Gutiérrez-Estrada<sup>3</sup>

Received: 8 February 2019 / Accepted: 12 November 2019  
© The Japan Society of Naval Architects and Ocean Engineers (JASNAOE) 2019

## Abstract

Fisheries management is generally based on the regulation of the fishing effort, by limiting fishing capacity and activity. The fishing capacity can be quantified objectively, however, the calculation of the fishing activity requires knowing the effective fishing time, for which it is essential to monitor the vessels activity. The European Vessel Monitoring System (VMS) only describes the geographical position, course and speed of the vessel at 2-h intervals, it is an expensive system used only in vessels over 12 m in length and there are no common criteria to infer the fishing activity from the VMS data. To evaluate more precisely the fishing activity, we propose to incorporate new sensors in the vessels that provide additional information. The sensors of mobile devices offer an economic solution that would allow their implementation throughout the fishing fleet. The objective of this work is to evaluate whether the most common sensors integrated in current mobile devices: GPS, accelerometer, gyroscope, and magnetic field, offer relevant information to identify the different phases of bottom trawling fishing activity. The results obtained indicate that these sensors detect, with very high precision, foreseeable changes in the movement of the vessel during the towing manoeuvre.

**Keywords** Vessel monitoring system · Mobile device · Sensor · Trawl fishing · Ship's behaviour

## 1 Introduction

The sustainable exploitation of fishery resources is based on the use of common indicators to measure fishing activity [1]. The European Union, under the Common Fisheries Policy, continuously analyses how to improve the fishing capacity and effort indicators of its fishing fleet [2]. The

fishing capacity can be objectively quantified from the vessels' technical characteristics and the fishing gears; however, the calculation of the fishing activity requires knowing the effective fishing time [3]. Therefore, an accurate estimate of the fishing effort requires knowing the time when the fishing gear is working, for which it is essential to monitor the vessels' activity.

With the aim of improving the effectiveness and efficiency of monitoring, control and surveillance of fishing activity, the European Union regulated in 2009 the use of vessel monitoring system (VMS) [4]. Thus, from January 1, 2012, every vessel with a total length of more than 12 m has a VMS transmitter installed, which provides each State Fishing Monitoring Centre with real-time information on the geographical position, course and speed of the vessel.

VMS data have become an indispensable tool to research on the control and planning of fishing activity [5, 6]. For example, they have been used to complete and verify the information provided by the electronic recording and reporting system (ERS) and to establish spatial and temporal maps of fishing activity, to study patterns of fishermen's behaviour [7] as well as to accurately assess the vessels' trajectories [8–14]. Several authors such as Lee [15] and Szostek [16] have developed and validated fishing effort estimation

✉ M. M. Galotto-Tebar  
m.galotto@umh.es  
A. Pomares-Padilla  
pomares@umh.es  
I. A. Czerwinski  
ivone.czerwinski@uca.es  
J. C. Gutiérrez-Estrada  
juanc@uhu.es

<sup>1</sup> Dpto. de Ingeniería de Computadores, Universidad Miguel Hernández, Campus de Elche, Avenida del ferrocarril s/n, 03202 Elche, Alicante, Spain  
<sup>2</sup> Dpto. de Biología, Facultad de CC. del Mar y Ambientales, Universidad de Cádiz, Campus de Puerto Real, 11510 Puerto Real, Cádiz, Spain  
<sup>3</sup> Dpto. de Ciencias Agroforestales, Escuela Técnica Superior de Ingeniería, Campus de El Carmen, Universidad de Huelva, 21007 Huelva, Spain

methods based on the recorded VMS data in United Kingdom vessels. On the other hand, Marzuki [17] used the VMS data for the monitoring and identification of unauthorised fishing activities. In this sense, Gerritsen [5] analysed the effects on CPUE (catch per unit of effort) of the seasonal closure of cod (*Gadus morhua*) from the VMS data. Currently the information provided by the VMS is available on platforms such as those developed in the Global Fishing Watch projects whose purpose is to provide a tool that allows governments, fishery management organisations, scientists, private industry, and non-governmental organisations to implement rules and regulations that will ensure a sustainable and abundant ocean ([www.globalfishingwatch.org](http://www.globalfishingwatch.org)).

Despite the undoubted advantages of the availability and use of VMS data, there are certain aspects that hinder to interpret the information they provide. In the first place, as indicated in [4], the installation of transponders is only mandatory for vessels with a length exceeding 12 m, so that the information coming from a large part of the artisanal fleet is not available. On the other hand, the information transmitted is relatively scarce since the devices send data with a very low frequency (intervals of at least 2 h) limiting the reliability and precision of the obtained results. Likewise, the use of the VMS data for the determination of trajectories, spatial and temporal fishing maps, and estimation of the fishing effort requires a validation with the auxiliary information provided by the logbooks and/or the on board observers reports [11]. Another VMS deficiency is that it does not provide information on the state of the sea to assess its influence on the trawl gear performance [18] and improve the fishing effort estimation. In addition, the VMS only provides the vessel's speed over the ground and does not report the vessel's true speed over the surface, obtaining erroneous results in areas with high sea currents. Therefore, we think that to evaluate fishing effort more accurately, it is necessary to develop new devices that provide better quality information and whose cost favours their implementation throughout the fishing fleet.

Considering that the presence of an active trawl gear affects the dynamic behaviour of the vessel, as it is affirmed and mathematically modelled by Sun [19], a device equipped with sensors and sufficient processing capacity could record the movement of the vessel and identify the different phases of fishing activity. This task could be carried out by a mobile device (tablet or Smartphone), thanks to the sensors it usually incorporates, its high processing capacity and facility for the development of specific applications (APP). At present, there are many fishing APPs, most of them for sport fishing, which take advantage of the sensors potential to georeference the fishing activity. For example, Fishing Status (<https://play.google.com/store/apps/details?id=com.FishingStatus>) is an application that provides resources and information (local fishing reports and hotspots with GPS

coordinates) around 100 miles of the current device location. For its part, Fishing Log (<https://play.google.com/store/apps/details?id=com.WebAndPrint.FishDiary>) is a logbook application that uses the GPS to georeference the information. Therefore, from the technical point of view, we consider it interesting to explore the use of mobile devices on the control and planning of fishing activity.

The objective of this work is to evaluate if the most common sensors integrated in current mobile devices: GPS, accelerometer, gyroscope and magnetic field are capable of offering relevant information that allows the identification of the different phases of fishing activity.

## 2 Materials and methods

### 2.1 Mobile device, sensors, variables and data

Nowadays, most mobile phones and tablets incorporate GPS, accelerometer, gyroscope and magnetic field sensors. In this work, we used a Samsung SM-P600 tablet with a 6-axis inertial sensor (Bosch Sensortec BMI055) consisting of a digital tri-axial 12 bit acceleration sensor and a digital tri-axial 16 bit gyroscope, a 3-axis electronic 16 bit compass sensor (Asahi Kasei Microdevices AK8963C) and a GPS receiver. From these sensors, a total of 11 variables can be obtained with a sampling period ranging from 50 ms to 1 s (Table 1).

The accelerometer measures the acceleration applied to the device ( $\overline{A_{ce}}$ ). Conceptually, it does so by measuring forces (F) applied to the mass of the sensor. In particular, the force of gravity ( $\vec{G}$ ) is always influencing the measured acceleration (Eq. 1). By immobilising the device on the vessel, it moves in solidarity with the vessel, so the mass of the equation corresponds to the sum of the mass of the device plus that of the vessel and this term can be disregarded and consider that the accelerometer will record the components of the gravity vector ( $\vec{G}$ ) at each instant:

$$\overline{A_{ce}} = -\vec{G} - \sum \vec{F}/\text{Mass} \approx -\vec{G}. \quad (1)$$

The gyroscope measures, in radians per second (rad/s), the rotation speed around the axes OX, OY and OZ being positive, when the rotation around the axis is made in the anticlockwise direction seen by an observer located in a positive location of the axis.

For its part, the magnetic field sensor measures, in micro-Teslas ( $\mu\text{T}$ ), the magnetic field in the device environment. The sensor provides the vector components resulting from the vector sum of the earth's magnetic field and the magnetic field generated by the objects in the environment (motors, wiring, etc.) (Eq. 2):

**Table 1** Main characteristics of the sensors used, description of the recorded physical parameter, data generation interval of each sensor (sampling period) and variables extracted from each parameter

Sensor	Measured parameter	Sampling period	Variable
Acceleration	Linear acceleration vector	50 ms	AceX AceY AceZ
Range = $\pm 19.6133 \text{ m/s}^2$ Sensitivity = $0.009570 \text{ m/s}^2$			
Gyroscope	Rotation speed around the three axes	50 ms	GirX GirY GirZ
Range = $\pm 8.7266 \text{ rad/s}$ Sensitivity = $0.0002661 \text{ rad/s}$			
Magnetic field	Vector of the magnetic field	50 ms	MagX MagY MagZ
Range = $\pm 4900 \mu\text{T}$ Sensitivity = $0.6 \mu\text{T}$			
GPS	Bearing	1 s	GpsR
	Speed		GpsV

$$\vec{\text{Mag}} = \vec{\text{Mag}}_{\text{Earth}} + \vec{\text{Mag}}_{\text{Environ}} \quad (2)$$

Finally, the GPS (global positioning system) sensor is capable of recording information about its three-dimensional geographic location in the form of latitude, longitude and height based on a satellite network. It also registers a temporary mark of the measurement and generates additional processed information such as course and instantaneous speed, average speed and precision. In this work, it has only been considered necessary to store the bearing (GpsR) and the instantaneous speed (GpsV) every second during the vessel activity.

## 2.2 The mobile application

A mobile application (APP) has been developed to record the vessel's movement during its fishing activity. The integrated development environment (IDE) Android Studio has been used to implement the APP on the Android platform. The user interface allows to start the recording and to select the haul phase. Once the recording has begun, the interface shows the data recorded by the sensors numerically and graphically. In addition, it incorporates a configuration menu with data about the ship, the mobile device and the fishing gear. During the recording, the data provided by the sensors, linked to the haul phase, ship's information, fishing gear and mobile device, are temporarily stored in a local database (SQLite).

The communication with the mobile device is done through a REST API ("Application Programming Interface for the Representational State Transfer") service. When the mobile device has a connection to the server, it sends the information temporarily stored in its database and the server stores it in a MySQL database (Fig. 1). The server allows access to information through the REST API service or through the WEB service using the RStudio application (Fig. 2).

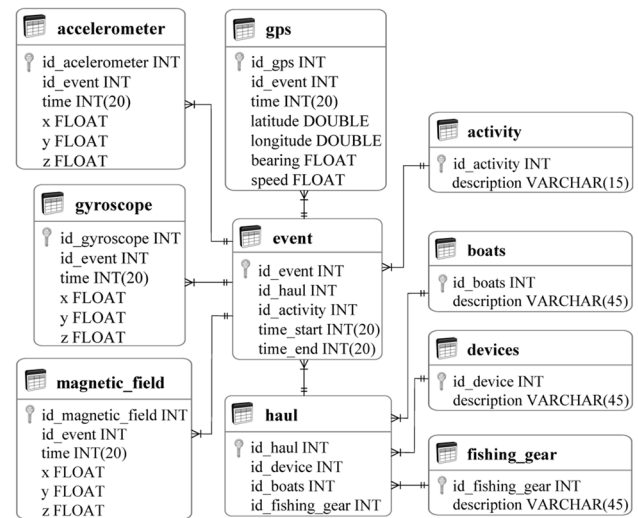


**Fig. 1** Structure of the relational database that stores the data recorded by the sensors of the mobile device. The accelerometer table contains the acceleration applied to the mobile device (vector  $\{x,y,z\}$ ) and the instant (time) in which it has been recorded. The gyroscope table contains the rotation speed around the three axes (vector  $\{x,y,z\}$ ) of the mobile device and the instant (time) in which it was recorded. The magnetic field table contains the magnetic field around the mobile device (vector  $\{x,y,z\}$ ) and the instant (time) in which it has been recorded. The GPS table contains the position (latitude and longitude), bearing and speed of the vessel and the instant (time) in which it has been recorded. The activity table contains the description of the four different activities of the vessel: shipping, setting, towing and hauling. The boats table contains the description of the fishing vessels involved in the study. The devices table contains the description of the mobile device used. The fishing gear table contains the description of the fishing gear used. Table haul contains the registered haul number. The event table allows to relate each data stored in the accelerometer, gyroscope, magnetic field and GPS tables to the activity, haul number, fishing vessel, fishing gear and mobile recording device





Fig. 2 Mobile application user interface and information flow

### 2.3 Case study

The initial execution of the prototype was carried out on the fishing and oceanographic research vessel Miguel Oliver [20] of the General Fisheries Secretariat of Spain, with one length of 70.00 m, beam of 14.40 m, draft of 6.50 m, gross register tonnage of 2.495 GT, maximum speed of 14 knots and equipped with a small draft trawl GOC-73 with Morguere doors. The data survey was performed in 2016 during the MEDITS-ES [21] survey conducted annually by the Spanish Institute of Oceanography (IEO) to evaluate demersal resources along the continental shelf and slope of the Spanish Mediterranean coast from May 27 to June 5, 2016 in the coasts of Castellón, Tarragona, Barcelona and Gerona (Fig. 3). During the campaign, the ship movement was recorded along 22 trawl hauls, at 3 knots speed, distributed in 20 sets of 30 min in depths from 50 to 200 m, two sets of 60 min in depth greater than 200 m and an average capture of 60 kg. In each set, it was recorded at least 15 min before the haul (shipping), the complete periods of setting, towing and hauling, and 15 min shipping after the haul.

To record as accurately as possible, the roll and pitch of the ship, the device was placed on the bridge about 18 m above the ship's centre of gravity, crossing point of the pitch and roll axes [22]. Special interest was placed on the orientation of the device as the sensors offer vector information referenced to the coordinate axes linked to the screen, placing the axis OY parallel to the longitudinal axis (stern-bow), the axis OX parallel to the transverse axis (port-starboard) and the OZ axis parallel to the vertical axis (Fig. 4).

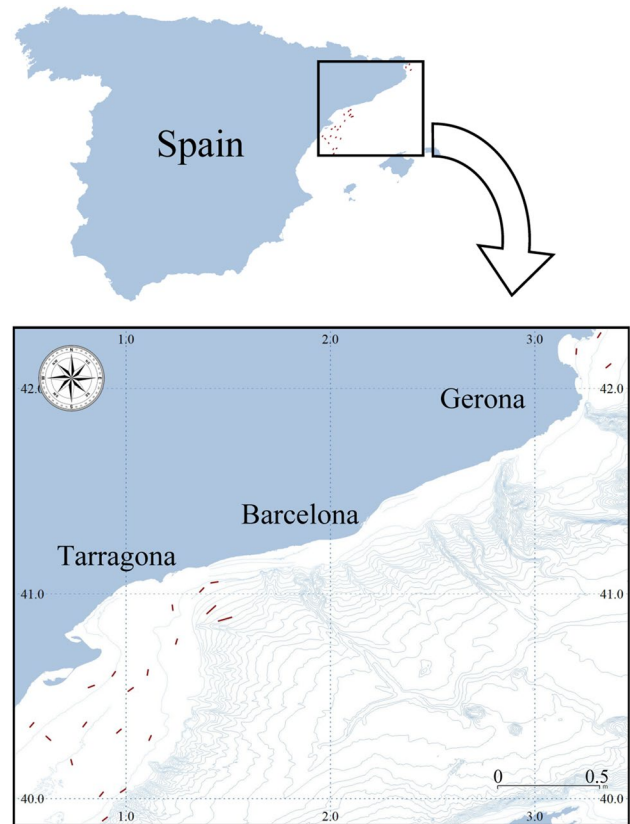


Fig. 3 Spatial distribution of the 22 hauls recorded along the coast of Castellón, Tarragona, Barcelona and Gerona (Spain)

### 2.4 Data analysis

From the information recorded by the sensors and stored in the database, the data table was made by estimating the mean ( $X_m$ ) and the standard deviation ( $X_s$ ) in 1-min periods,

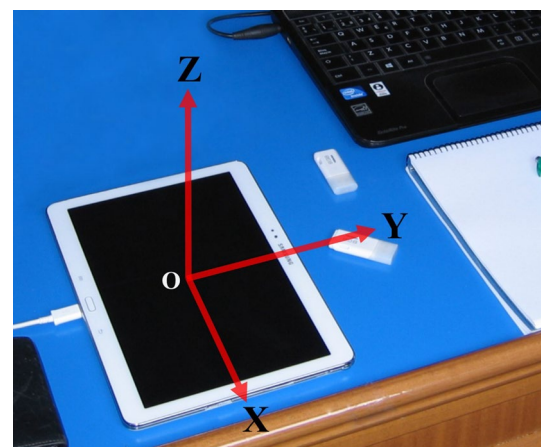


Fig. 4 Location of the mobile device on the bridge of the oceanographic vessel

thus obtaining 22 independent quantitative continuous variables. Likewise, a nominal qualitative independent variable named *Activity* composed of four categories (shipping, shooting the gear, towing and hauling the gear) was created. The data table was formed by 22 variables with 2453 data divided into 1140 shipping, 262 during the gear shooting, 786 towing and 265 during the gear hauling.

The data analysis focused on identifying the changes in the static and dynamic vessel behaviour during the haul, in identifying the sensors capable of measuring those changes, in locating the quantitative variables to be used to recognise said changes, and in analysing the variables behaviour in the different haul phases. Each quantitative variable was analysed using the kurtosis and Fisher's asymmetry coefficients, the Shapiro–Wilk test to contrast the normality, the box and density plots by haul phase to observe differences, their median and interquartile range by haul phase to detect differences in its central value and dispersion, its coefficient of variation of the absolute deviation of the median (MAD) to discard unrepresentative variables and the non-parametric test of Kruskal–Wallis to confirm the differences between the median values by haul phase. Likewise, quantitative variables were standardised to compare them with each other. The statistical package RStudio was used to perform all the analyses.

### 3 Results

This section shows the obtained results from the data table variables related to the trim of the ship and the four degrees of freedom of movement affected by the start of the haul and susceptible to be registered by the available sensors: pitch, roll, yaw and surge.

#### 3.1 Trim

The presence of an active fishing gear causes changes in the ship's trim, modifying the angle formed by its longitudinal axis with the horizontal plane. The accelerometer is the sensor capable of recording information about the ship's orientation. The variables  $AceX_m$ ,  $AceY_m$  and  $AceZ_m$  represent the mean gravity vector components and provide information on the ship's orientation with respect to the horizontal plane. The projection of the gravity vector on the centreline plane, represented by the variables  $AceY_m$  and  $AceZ_m$ , makes it possible to evaluate the longitudinal angle of the ship trim.

The variable  $AceY_m$  showed a value of kurtosis ( $\beta=4.27$ ) and a  $p$  value of the Shapiro–Wilk test ( $p<0.001$ ) that suggested that the data did not adjust to a normal distribution. The Kruskal–Wallis test ( $p<0.001$ ) showed the existence of significant differences in its central value and dispersion between activities. During the set, their median increased

by 42% and their interquartile range was reduced by 58% (Table 2, Fig. 5). On the other hand,  $AceZ_m$  presented a clearly non-normal behaviour ( $\gamma=2.74$ ,  $\beta=21.58$ , Shapiro–Wilk test  $p<0.001$ ) and its density by activity showed the absence of significant differences in its central value and dispersion (Kruskal–Wallis test  $p=0.749$ ) (Table 2; Fig. 6).

#### 3.2 Roll and pitch

Pitch and roll movements are originated by external forces such as waves, wind, etc. In both cases, the vessel describes the rotational movements around its transverse and longitudinal axis, causing the alternate rise and fall of the bow and stern or of the port and starboard bands. The presence of an active fishing gear causes the displacement of the vessel mass centre (crossing point of the transverse and longitudinal axes) and modifies the pitch and roll movements. The accelerometer, gyroscope and magnetic field sensors detect these changes.

The accelerometer showed higher values of the coefficient of variation in  $AceX_s$ ,  $AceY_s$  and  $AceZ_s$ . Like  $AceZ_m$ , the deviations associated with the three axes of the accelerator present behaviours with non-normal distributions. In  $AceX_s$  and  $AceZ_s$  (Kruskal–Wallis  $AceX_s$  test  $p<0.001$ ; Kruskal–Wallis  $AceY_s$  test  $p=0.168$ ; Kruskal–Wallis  $AceZ_s$  test  $p<0.001$ ) (Table 2; Figs. 7, 8).

The gyroscope measures the speed of rotation around the  $X$ ,  $Y$  and  $Z$  axes. The sensors orientation on the ship indicates that the variable  $GirX$  records the pitch movement and the variable  $GirY$  the roll movement. In particular, the  $GirX_s$  and  $GirY_s$  variables of the data table must change in the variability or dispersion of the pitch and roll rotation speed. The  $GirX_s$  and  $GirY_s$  components showed a non-normal behaviour and at least one of them ( $GirY_s$ ) pointed out the possibility of differentiating the navigation from the towing, shooting and hauling activities (Kruskal–Wallis  $GirY_s$  test  $p<0.001$ ) (Table 2; Fig. 9), however,  $GirX_s$  did not present any difference between the four activities (Kruskal–Wallis test  $GirX_s$   $p=0.198$ ).

For its part, the magnetic field sensor measures in micro-Teslas ( $\mu T$ ), the magnetic field in the environment of the device. Therefore, all the components of the vector that register the sensor ( $MagX$ ,  $MagY$  and  $MagZ$ ) and particularly the variables  $MagX_s$ ,  $MagY_s$  and  $MagZ_s$  are likely to show the pitch and roll changes in the different haul phases. The Shapiro–Wilk tests indicate that none of the three variables presented a normal distribution. However, a comparison of medians showed differences between the central value and the dispersion between shipping and towing activities in the variables  $MagX_s$ ,  $MagY_s$  (Kruskal–Wallis  $MagX_s$  test  $p<0.001$ ) (Table 2, Figs. 10 and 11) and to a lesser extent in the variable  $MagZ_s$ .

**Table 2** Statistical summary of the 22 variables under study

	AceX <sub>m</sub>	AceY <sub>m</sub>	AceZ <sub>m</sub>	GirX <sub>m</sub>	GirY <sub>m</sub>	GirZ <sub>m</sub>	MagX <sub>m</sub>	MagY <sub>m</sub>	MagZ <sub>m</sub>	GpsR <sub>m</sub>	GpsV <sub>m</sub>
<i>N</i>	2453	2453	2453	2453	2453	2453	2453	2453	2453	2453	2453
Mean	− 1.0302	0.0412	9.8941	− 0.0001	0.0003	0.0000	− 29.2530	60.0077	− 15.2240	140.8623	4.9530
Median	− 1.0420	0.0440	9.8940	0.0000	0.0000	0.0000	− 33.5270	65.4720	− 16.0900	114.2770	3.4580
SD	0.0692	0.0162	0.0121	0.0005	0.0005	0.0027	11.6915	15.1598	3.0334	103.6299	2.9446
CV_Pearson	0.0672	0.3932	0.0012	4.7825	1.4049	62.8112	0.3997	0.2526	0.1992	0.7357	0.5945
MAD	0.0667	0.0163	0.0074	0.0000	0.0000	0.0000	12.7593	17.3242	2.8807	116.2092	1.5879
CV_MAD	0.0640	0.3707	0.0007	−	−	−	0.3806	0.2646	0.1790	1.0169	0.4592
Min	− 1.4660	− 0.0420	9.8300	− 0.0040	− 0.0010	− 0.0270	− 50.0170	34.9760	− 20.8220	2.6130	0.0580
Max	− 0.6170	0.0870	9.9930	0.0020	0.0020	0.0240	− 6.8830	81.2610	− 7.5720	356.0770	10.3920
Range	0.8490	0.1290	0.1630	0.0060	0.0030	0.0510	43.1340	46.2850	13.2500	353.4640	10.3340
Skewness	0.3780	− 0.8532	2.7354	− 1.7448	0.7071	0.0192	0.4113	− 0.3437	0.6319	0.5513	0.6494
Kurtosis	4.2573	4.2739	21.5804	14.2086	1.6542	36.7724	1.6587	1.5022	2.4319	2.0463	1.9805
Kr.Wallis <i>p</i> val	0.1177	0.0000	0.7489	0.0158	0.9760	0.0001	0.0000	0.0000	0.0000	0.0000	0.0000
	AceX <sub>s</sub>	AceY <sub>s</sub>	AceZ <sub>s</sub>	GirX <sub>s</sub>	GirY <sub>s</sub>	GirZ <sub>s</sub>	MagX <sub>s</sub>	MagY <sub>s</sub>	MagZ <sub>s</sub>	GpsR <sub>s</sub>	GpsV <sub>s</sub>
<i>N</i>	2453	2453	2453	2453	2453	2453	2453	2453	2453	2453	2453
Mean	0.0872	0.0680	0.0645	0.0039	0.0032	0.0019	0.4904	0.5637	0.4417	7.6063	0.2339
Median	0.0680	0.0540	0.0490	0.0030	0.0020	0.0020	0.3290	0.4030	0.3940	1.0430	0.0690
SD	0.0568	0.0395	0.0450	0.0019	0.0020	0.0013	0.7251	0.7283	0.3198	22.0062	0.4935
CV_Pearson	0.6516	0.5815	0.6973	0.4818	0.6135	0.6631	1.4785	1.2921	0.7240	2.8931	2.1097
MAD	0.0356	0.0297	0.0282	0.0015	0.0015	0.0015	0.0593	0.0771	0.1097	0.9563	0.0474
CV_MAD	0.5233	0.5491	0.5749	0.4942	0.7413	0.7413	0.1803	0.1913	0.2785	0.9169	0.6876
Min	0.0180	0.0090	0.0150	0.0020	0.0010	0.0010	0.2330	0.2820	0.2540	0.1040	0.0000
Max	0.4170	0.2610	0.3350	0.0130	0.0150	0.0140	16.2410	16.8470	11.6380	179.0620	4.3130
Range	0.3990	0.2520	0.3200	0.0110	0.0140	0.0130	16.0080	16.5650	11.3840	178.9580	4.3130
Skewness	1.8170	1.2624	1.9776	1.0152	1.9266	3.5891	9.6756	9.3140	20.9884	4.8946	4.5567
Kurtosis	6.9348	4.2777	7.8477	3.5099	7.5787	23.9303	140.6254	139.7816	653.1549	29.7713	28.2055
Kr.Wallis <i>p</i> val	0.0000	0.1677	0.0000	0.1977	0.0000	0.0000	0.0000	0.0000	0.0000	0.0000	0.0000

The variable with subscript *m* represents the average of the data generated by the sensor in periods of 1 min. The variable with subscript *s* represents the standard deviation of the data generated by the sensor in periods of 1 min. For each variable, the table includes the number of samples (*N*), the mean, the median, the standard deviation (SD), the Pearson's Coefficient of Variation (CV\_Pearson), the median absolute deviation (MAD), the coefficient of variation of the median absolute deviation (CV\_MAD), the minimum value (min), the maximum value (max), the range of values (range), the skewness, the kurtosis and the *p* val of the Kruskal–Wallis normality test (Kr.Wallis *p* val) double

### 3.3 Yaw

The yaw movement is a rotation oscillatory movement around the ship OZ axis that causes small changes in the course of the vessel. The sensors capable of recording the yaw are the gyroscope, the magnetic field sensor and the GPS.

The Z component of the gyroscope measures the speed of rotation around the OZ axis and the variable GirZ<sub>s</sub> records the magnitude of the course changes during the fishing activity. The GirZ<sub>s</sub> data had a clearly asymmetric distribution ( $\gamma=3.59$ ) that caused the Shapiro–Wilk test to be highly significant ( $p<0.001$ ). Likewise, it showed a high variability around its median, which was reflected in the level of significance of the Kruskal–Wallis test ( $p<0.001$ ) (Table 2, Fig. 12).

In turn, the magnetic field sensor *X* and *Y* components are the most sensitive ones to the ship yaw along with the variables described in the previous section MagX<sub>s</sub> and MagY<sub>s</sub> that reflect its magnitude.

The GPS sensor provided also information on vessel the course and speed. GpsR<sub>s</sub> is the more sensitive to yaw variable. This variable showed a high variability of 92% around its median (Table 2). The density diagram (Fig. 13) showed significant differences in its central value and dispersion among activities (Kruskall–Wallis test  $p<0.001$ ). Its median decreased by 16% in the shooting phase, increased by 53% in the towing phase and by 160% in the hauling phase.



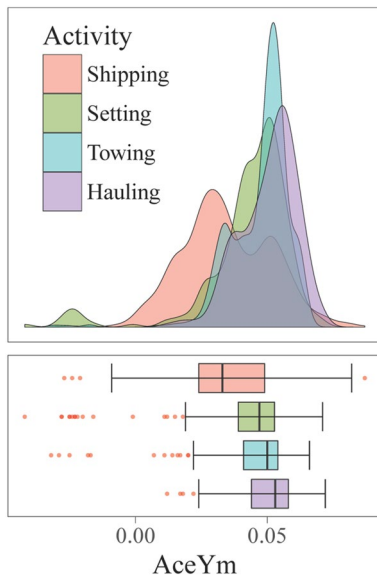


**Fig. 5** Tukey boxplots and density by activity of the variable  $AceY_m$

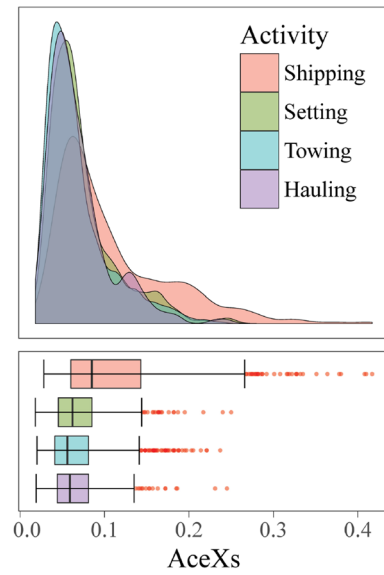


**Fig. 7** Tukey boxplots and density by activity of the variable  $AceX_s$

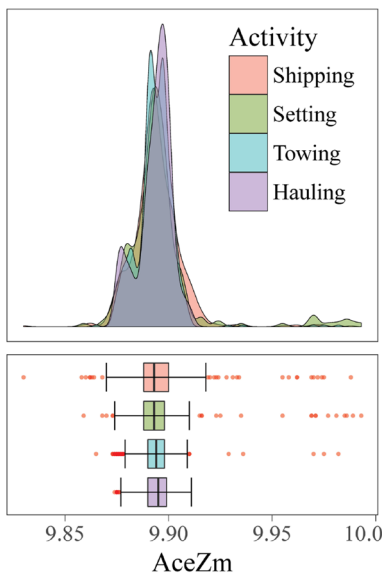


**Fig. 6** Tukey boxplots and density by activity of the variable  $AceZ_m$

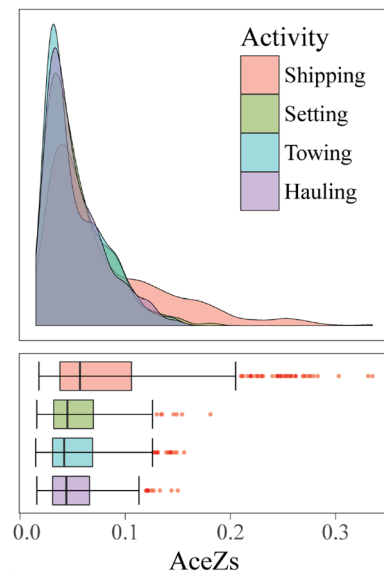


**Fig. 8** Tukey boxplots and density by activity of the variable  $AceZ_s$

### 3.4 Surge

The study of the surge speed during the different fishing activity phases focuses on analysing the average speed and speed stability against external forces. In this way, the sensor that measures the surge speed is the GPS and  $GpsV_m$  is the variable to show the average speed evolution. This variable clearly discriminates between the navigation and the rest of the activity phases and this was reflected in significant differences of its central value and dispersion (Table 2; Fig. 14).

On the other hand, the surge stability is characterised by the variable  $GpsV_s$  (speed variability). The analysis of this variable indicated that both, the asymmetry and kurtosis coefficients, were out of range ( $\gamma=4.56$ ,  $\beta=28.21$ ). A Shapiro–Wilk test ( $p<0.001$ ) confirmed that the data did not show a normal distribution. The variable showed a high variability of 69% around its median (Table 2). The activity density (Fig. 15) and the Kruskal–Wallis test ( $p<0.001$ ) showed significant differences in their central value and dispersion among the activities. Its median decreased by 24% in the towing phase and increased by 125% in the shooting phase and by 62% in

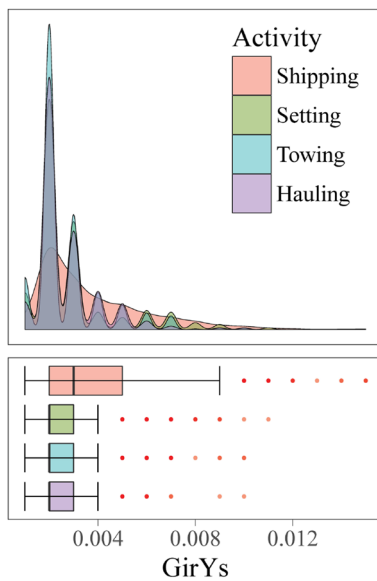


**Fig. 9** Tukey boxplots and density by activity of the variable  $GirY_s$

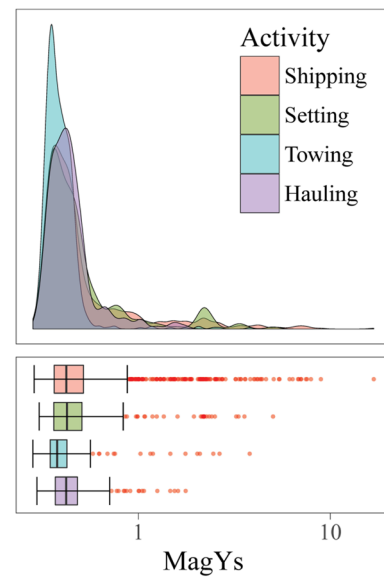


**Fig. 11** Tukey boxplots and density by activity of the variable  $MagY_s$ . Logarithmic scale was used on the OX axis

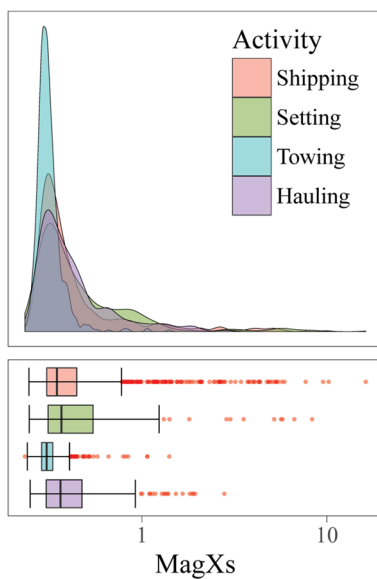


**Fig. 10** Tukey boxplots and density by activity of the variable  $MagX_s$ . Logarithmic scale was used on the OX axis

the hauling phase. Its interquartile range decreased by 33% in the towing phase and increased by 267% in the shooting phase and by 93% in the hauling phase.

## 4 Discussion

Significant progress in data collection involves the acquisition of this information for all vessels, including those that are not required to have a VMS system installed, for which it

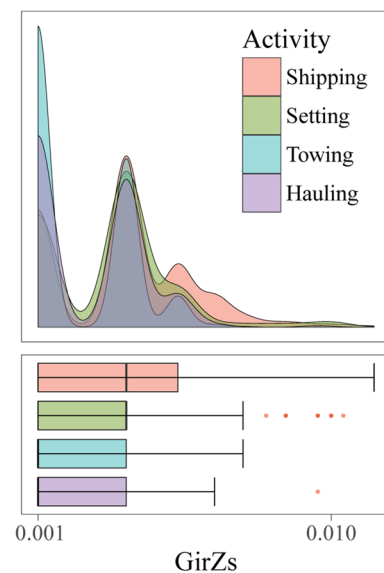


**Fig. 12** Tukey boxplots and density by activity of the variable  $GirZ_s$ . Logarithmic scale was used on the OX axis

is essential to develop effective, low-cost and easy-to-install systems. Faced with the high cost of current VMS devices, the solution we propose for each fishing vessel is a mobile device running a specific APP and a modem that allows its connection to a satellite network. In the coastal fleet, the cost can be reduced if the communication is done through the mobile phone network or using the WiFi network, when arriving at the port. The estimation of the cost has been calculated using a medium-range mobile phone and an Iridium

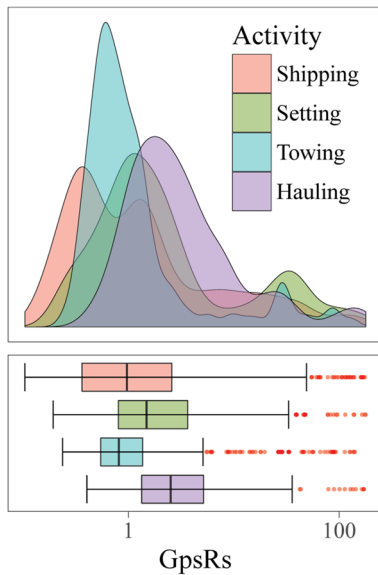


**Fig. 13** Tukey boxplots and density by activity of the variable  $GpsR_s$ . Logarithmic scale was used on the OX axis

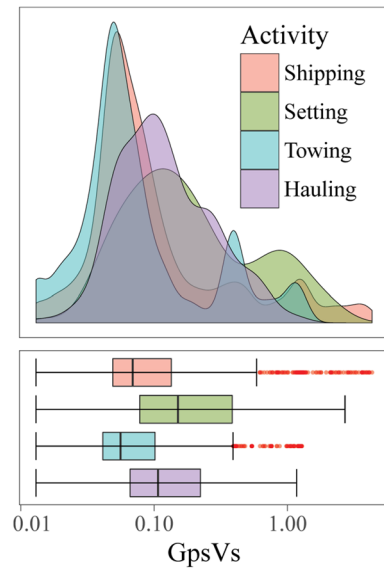


**Fig. 15** Tukey boxplots and density by activity of the variable  $GpsV_s$ . Logarithmic scale was used on the OX axis

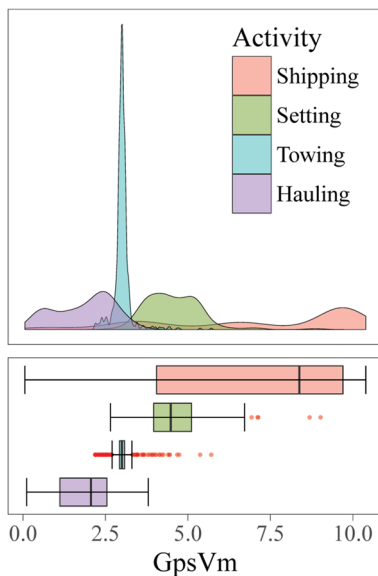


**Fig. 14** Tukey boxplots and density by activity of the variable  $GpsV_m$

modem with worldwide coverage, obtaining an estimated cost of 700 € for local equipment and 400 €/year of maintenance and data transmission. These numbers contrast with the current costs of the VMS for deep-sea fishing of 3500 € for local equipment and 800 €/year of maintenance, or the costs for coastal fishing such as the SLSEPA system of 1400 € for local equipment and 1200 €/year of maintenance [23].

To evaluate if the sensors of mobile devices have the necessary sensitivity to record changes in the movement of the vessel when the trawl is active, we found the most

unfavourable test environment, where these changes were minimal. The effect of the trawl fishing gear on the vessel depends on the size of the vessel, the size of the fishing gear and the volume of catch dragged [19]. On the one hand, the larger the vessel, the smaller the movement due to wind and waves. On the other hand, the smaller the fishing gear and the volume of catch with respect to the size of the vessel, the smaller its effect on the vessel and the differences in the dynamic behaviour of the vessel between each phase of the fishing set will be smaller. The oceanographic vessel Miguel Oliver during the Medits campaign meets these requirements, it is a large vessel equipped with a small sampling trawl, executing during the campaign sets of short duration and with a small volume of catch. A commercial trawler usually offers more favourable conditions for sensors to record differences in their dynamic behaviour during the set. Therefore, we can state that the results presented in this paper can be applied to most of the trawl fishing fleet. These results are analysed below.

#### 4.1 Trim

During the set, the fishing gear is towed by two cables located on both sides of the stern of the vessel, each one exerting a pulling force on the vessel that causes changes in its static and dynamic behaviour [19]. This force appears when the gear is released, increases during the trawling phase and is maximal when the trawling speed increases during the hauling phase. The vertical component of these forces causes a progressive ship centre of mass displacement aft and consequently an increase in the ship seat.

## 4.2 Pitch and roll

When a ship is in equilibrium position, the centre of buoyancy (point through which the force of buoyancy supporting the vessel acts vertically upwards) and the centre of gravity (point through which all of the weight of the vessel acts vertically downwards) are in the same vertical axis. When an external force inclines the ship, the submerged part of the hull is modified; the centre of the hull moves and a righting pair that opposes this inclination is generated [22, 24].

The presence of a fishing gear increases the righting torque and reduces the vessel pitch and roll [19]. In both movements, there are variations in speed and drag that cause an additional centre of masses displacement increasing its distance from the centre of the hull.

Our results show that the accelerometer, gyroscope and magnetic field sensors were able to detect a decrease in the pitch and roll level during the haul. In the case of the accelerometer, the variables  $AceX_s$  and  $AceZ_s$  reflected a significant reduction in their median and interquartile range. On the other hand, the  $GirY_s$  gyroscope variable reflected a reduction of its median and interquartile range. Finally, the  $MagX_s$  and  $MagY_s$  magnetic field sensor variables recorded a reduction in its median and interquartile range during the towing phase.

## 4.3 Yaw

The yaw movement is a rotation oscillatory movement around the ship's OZ axis that causes small changes in the vessel's course. A starboard turn accelerates the port drag line and slows the starboard line, causing an imbalance in the drag forces that opposes the ship's turn. A turn to port provokes the same effect. As a result, during the haul, the yaw movement is reduced and the ship's course remains more stable [19].

The gyroscope, the magnetic field sensor and the GPS have been able to detect the reduction of the yaw angle during haul. In the case of the gyroscope, the  $GirZ_s$  variable has shown a reduction in the towing phase in its median and interquartile range. As mentioned in the previous section, the  $MagX_s$  and  $MagY_s$  variables of the magnetic field sensor have also shown greater stability on the course during the haul. Finally, the results obtained with the GPS indicate that the variable shows small reductions of its median and a significant reduction of its interquartile range between the shipping and towing phases. During the setting and hauling phases, there is an increase of this movement due to the fact that in these phases, there are usually course changes to orient the vessel to the haul that will begin or to direct the vessel to the next fishing zone.

## 4.4 Surge

The study of the ship speed during the different fishing activity phases focuses on analysing the average speed reached voluntarily by acting on the propulsion system and observing the stability of the desired speed against external forces (waves, gusts of wind, etc.).

The variable  $GpsV_m$  reflected, in each haul phase, velocity values similar to those found in other studies for trawl fishing [15, 17, 25], with medians of 8.4 knots shipping, 4.5 knots setting, 3 knots towing and 2.1 knots hauling. Furthermore, the expected variability of the speed is reflected in its interquartile ranges of 5.7 knots shipping, 1.2 knots setting, 0.16 knots towing and 1.4 knots hauling.

During the haul, small variations in speed cause changes in the drag force that opposes to the speed change. The trawl net shock absorbing effect allows the vessel to maintain a more stable forward speed [19]. The analysis of the variable  $GpsV_s$  data shows that the speed value and speed variation are lower in the towing phase than in the shipping phase. During the set and haul phases, the speed varies voluntarily, which justifies an increase in the  $GpsV_s$  median and dispersion.

## 5 Conclusions

Processing data into information and information into knowledge to optimise the decision-making process is one of the great challenges facing the managing bodies that plan the exploitation of fishery resources. In this context, the VMS system has become a relevant source of data, boosting research on the fishing activity control and planning as can be seen in Gerritsen [5] and Jennings [6]. In spite of this, the scarce information offered by the VMS system limits its future.

Analysing the results of this article, the proposal to use in the future, a mobile-like device to overcome the VMS systems seems more viable. As a first step, we have verified that the sensors of a mobile device are capable of detecting significant differences in the movement of the vessel, as stated and mathematically modelled by Sun [19]. The experience was realised under very unfavourable conditions, in a large tonnage oceanographic vessel, with a small fishing gear, a small catch volume, and in weather conditions that did not cause large movements of the vessel. In spite of this, the sensors of the mobile device recorded a progressive increase in the ship's seat, a reduction in the angle of balance, pitch and yaw, and an increase in the stability of surge and speed values according to the haul phase.

In short, the results of this work indicate that the mobile device's sensors have been able to detect, with a very high

accuracy level, the foreseeable changes in the movement of the vessel during the trawling manoeuvre.

## 6 Software availability

Name of software: FAMIS. Developers: Galotto-Tebar, M.M. Hardware requirements: Mobile device with Android 5.1 or higher. Programming languages: Java. Availability: The programme will be available up on request to Ms. Maria del Mar Galotto-Tebar.

**Acknowledgements** This work has been developed, thanks to the Spanish Institute of Oceanography (IEO) collaboration and especially to the Medits-2016 campaign head Mr. Antonio Esteban Acón who facilitated our boarding in the Miguel Oliver oceanographic vessel whose crew was especially supportive. Our greatest thanks to BQ Spain (<https://www.bq.com>) for the material and technical support and to the company SatLink (<http://satlink.es>) for the information provided. We would also like to thank the Miguel Hernández University professors: Miguel Onofre Martínez Rach, Maria Asunción Vicente Ripoll and César Fernández Peris for collaborating in writing the manuscript and in the APP development. Finally, I would like to thank the editor and reviewers of the Journal of Marine Science and Technology for their invaluable help in correcting and refining the content of this article.

## References

1. FAO Fishery Resources Division (1999) Indicators for sustainable development of marine capture fisheries. FAO Technical Guidelines for Responsible Fisheries. No 8. Rome, p 68. <http://www.fao.org/3/a-x3307e.pdf>
2. European Commission (2007) Communication from the commission to the council and the European Parliament on improving fishing capacity and effort indicators under the common fisheries policy. Brussels, 5.2.2007 COM(2007) 39 final. <http://eur-lex.europa.eu/legal-content/EN/TXT/PDF/?uri=CELEX:52007DC0039&from=LV>
3. de Souza EN, Boerder K, Matwin S, Worm B (2016) Improving fishing pattern detection from satellite AIS using data mining and machine learning. PLoS One 11:e0158248. <https://doi.org/10.1371/journal.pone.0158248>
4. Council Regulation (EC) No 1224/2009 of 20 November (2009). Establishing a Community control system for ensuring compliance with the rules of the Common Fisheries Policy, amending Regulations (EC) No. 847/96, (EC) No 2371/2002, (EC) No. 811/2004, (EC) No. 768/2005, (EC) No. 2115/2005, (EC) No. 2166/2005, (EC) No. 388/2006, (EC) No. 509/2007, (EC) No. 676/2007, (EC) No. 1098/2007, (EC) No. 1300/2008, (EC) No. 1342/2008 and repealing Regulations (EEC) No. 2847/93, (EC) No. 1627/94 and (EC) No. 1966/2006. Official Journal of the European Union, L343: 1–50. Strasbourg. <http://eur-lex.europa.eu/legal-content/EN/TXT/PDF/?uri=CELEX:32009R1224&rid=1>
5. Gerritsen HD, Lordan C, Minto C, Kraak SBM (2012) Spatial patterns in the retained catch composition of Irish demersal otter trawlers: high-resolution fisheries data as a management tool. Fish Res 129–130:127–136. <https://doi.org/10.1016/J.FISHRES.2012.06.019>
6. Jennings S, Lee J (2012) Defining fishing grounds with vessel monitoring system data. ICES J Mar Sci 69:51–63. <https://doi.org/10.1093/icesjms/fsr173>
7. Shepperson J, Murray LG (2016) Use of a choice-based survey approach to characterise fishing behaviour in a scallop fishery. Environ Modell Softw 86:116–130. <https://doi.org/10.1016/j.envsoft.2016.09.013>
8. Palmer MC (2008) Calculation of distance travelled by fishing vessels using GPS positional data: a theoretical evaluation of the sources of error. Fish Res 89:57–64. <https://doi.org/10.1016/J.FISHRES.2007.09.001>
9. Deng R, Dichmont C, Milton D, Haywood M, Vance D, Hall N, Die D (2005) Can vessel monitoring system data also be used to study trawling intensity and population depletion? The example of Australia's northern prawn fishery. Can J Fish Aquat Sci 62:611–622. <https://doi.org/10.1139/f04-219>
10. Mills CM, Townsend SE, Jennings S, Eastwood PD, Houghton CA (2007) Estimating high resolution trawl fishing effort from satellite-based vessel monitoring system data. ICES J Mar Sci 64:248–255. <https://doi.org/10.1093/icesjms/fsl026>
11. Bastardie F, Nielsen JR, Ulrich C, Egekvist J, Degel H (2010) Detailed mapping of fishing effort and landings by coupling fishing logbooks with satellite-recorded vessel geo-location. Fish Res 106:41–53. <https://doi.org/10.1016/j.fishres.2010.06.016>
12. Gerritsen H, Lordan C (2011) Integrating vessel monitoring systems (VMS) data with daily catch data from logbooks to explore the spatial distribution of catch and effort at high resolution. ICES J Mar Sci 68:245–252. <https://doi.org/10.1093/icesjms/fsq137>
13. Hintzen NT, Bastardie F, Beare D, Piet GJ, Ulrich C, Deporte N, Egekvist J, Degel H (2012) VMStools: open-source software for the processing, analysis and visualisation of fisheries logbook and VMS data. Fish Res 115–116:31–43. <https://doi.org/10.1016/J.FISHRES.2011.11.007>
14. Cojan M, Burgos C (2015) Análisis de la información proporcionada por los sistemas de localización vía satélite de la flota que explota la chirla (*Chamelea gallina*) en el Golfo de Cádiz sistemas de localización vía satélite de la flota que explota la chirla (*Chamelea gallina*). In: Teledetección: Humedales y Espacios. XVI Congreso de La Asociación Española de Teledetección, pp 550–553. [http://www.aet.org.es/congresos/xvi/XVI\\_Congreso\\_AET\\_actas.pdf](http://www.aet.org.es/congresos/xvi/XVI_Congreso_AET_actas.pdf)
15. Lee J, South AB, Jennings S (2010) Developing reliable, repeatable, and accessible methods to provide high-resolution estimates of fishing-effort distributions from vessel monitoring system (VMS) data. ICES J Mar Sci 67:1260–1271. <https://doi.org/10.1093/icesjms/fsq010>
16. Szostek CL, Murray LG, Bell E, Kaiser MJ (2017) Filling the gap: using fishers' knowledge to map the extent and intensity of fishing activity. Mar Environ Res 129:329–346. <https://doi.org/10.1016/J.MARENVRES.2017.06.012>
17. Marzuki MI, Garelo R, Fablet R, Kerbaol V, Gaspar P (2015) Fishing gear recognition from VMS data to identify illegal fishing activities in Indonesia. In: MTS/IEEE OCEANS 2015. Institute of Electrical and Electronics Engineers Inc, Genoa, pp 1–5. <https://doi.org/10.1109/OCEANS-Genova.2015.7271551>
18. Politis PJ, DeAlteris JT, Brown RW, Morrison AT (2012) Effects of sea-state on the physical performance of a survey bottom trawl. Fish Res 123–124:26–36. <https://doi.org/10.1016/J.FISHRES.2011.11.017>
19. Sun X, Yin Y, Jin Y, Zhang X, Zhang X (2011) The modelling of single-boat, mid-water trawl systems for fishing simulation. Fish Res 109:7–15. <https://doi.org/10.1016/J.FISHRES.2010.12.027>
20. Buque oceanográfico Miguel Oliver (2019) Ministerio de agricultura, pesca y alimentación. <https://www.mapa.gob.es/es/pesca/temas/proteccion-recursos-pesqueros/buques-secretaria-general/investigacion-pesquera-oceanografica/miguel-oliver/default.aspx>. Accessed on 24 Jul 2019 (Online)



21. Bertrand JA, Gil de Sola L, Papaconstantinou C, Relini G, Souplet A (2002) The general specifications of the MEDITS surveys. *Sci Mar* 66:9–17. <https://doi.org/10.3989/scimar.2002.66s29>
22. Ibrahim RA, Grace IM (2010) Modelling of ship roll dynamics and its coupling with heave and pitch. *Math Probl Eng* 2010:1–32. <https://doi.org/10.1155/2010/934714>
23. Agricultura y Pesca C (2010) Location and track system for Andalusian Fishing Vessels (SLSEPA) (Technical report). Junta de Andalucía. [http://www.faocopemed.org/pdf/reg\\_net\\_dbases/locationandtracksystemforandalusianfishingvessels\(slsepa\).pdf](http://www.faocopemed.org/pdf/reg_net_dbases/locationandtracksystemforandalusianfishingvessels(slsepa).pdf)
24. Romano A, Marasco A (2014) Fluid dynamics and ship motion. Birkhäuser, New York, pp 429–461. [https://doi.org/10.1007/978-1-4939-1604-7\\_13](https://doi.org/10.1007/978-1-4939-1604-7_13)
25. Burgos C, Gil J, del Olmo LA (2013) The Spanish blackspot seabream (*Pagellus bogaraveo*) fishery in the Strait of Gibraltar: spatial distribution and fishing effort derived from a small-scale GPRS/GSM based fisheries vessel monitoring system. *Aquat Living Resour* 26:399–407. <https://doi.org/10.1051/alr/2013068>

**Publisher's Note** Springer Nature remains neutral with regard to jurisdictional claims in published maps and institutional affiliations.

## Expert Systems With Applications

### Is the vessel fishing? Discrimination of fishing activity with low-cost intelligent mobile devices through traditional and heuristic approaches

<b>Manuscript Number:</b>	ESWA-D-20-06080R2
<b>Article Type:</b>	Full length article
<b>Keywords:</b>	Vessel monitoring system; mobile device; Sensor; trawl fishing; ship's behavior; Machine learning
<b>Corresponding Author:</b>	Maria del Mar Galotto-Tébar, PhD student Universidad Miguel Hernandez de Elche Elche, Alicante SPAIN
<b>First Author:</b>	Maria del Mar Galotto-Tébar, PhD student
<b>Order of Authors:</b>	Maria del Mar Galotto-Tébar, PhD student
	Alejandro Pomares Padilla, Ph.D
	Ivone Alejandra Czerwinski, Ph.D
	Juan Carlos Gutiérrez Estrada, Ph.D
<b>Abstract:</b>	Knowing the activity of fishing vessels accurately and in real time means a leap in quality in the management of fishing activity. This paper presents the development of a new comprehensive fisheries monitoring system (FAMIS) that can complement and overcome the limitations of current fishing vessel monitoring systems (VMS). FAMIS is developed on the basis of a low-cost mobile device with GPS sensors, accelerometer, gyroscope and magnetic field and integrates different statistical methods (discriminant functions) and heuristics (artificial neural networks and vectorial support machines) as techniques to classify the information recorded by the sensors of a mobile device during fishing activity. The results obtained with FAMIS indicate that, in general, heuristics have a high degree of discrimination of each of the phases of fishing operation and that, in particular, multilayer perceptrons (MLPs) are capable of correctly identifying 96.3% of towing phases using only GPS and gyro sensors.

*Departamento de Ingeniería de Computadores*  
UNIVERSIDAD MIGUEL HERNÁNDEZ  
Campus de Elche, Avenida del ferrocarril s/n, 03202 Alicante, SPAIN

Ms. Maria del Mar Galotto Tébar  
Phone and fax: 34 966 65 83 96, E-mail: m.galotto@umh.es

March 26, 2021

**Manuscript title:** Is the vessel fishing? Discrimination of fishing activity with low-cost intelligent mobile devices through traditional and heuristic approaches.

**Authors:** Maria del Mar GALOTTO-TÉBAR, Alejandro POMARES-PADILLA, Ivone Alejandra CZERWINSKI, Juan Carlos GUTIERREZ-ESTRADA.

Recommend Editor  
Dr. Binshan Lin  
Editor-in-Chief, Expert Systems with Applications

Dear Dr. Lin:

Please find enclosed one copy of the revised manuscript "Is the vessel fishing? Discrimination of fishing activity with low-cost intelligent mobile devices through traditional and heuristic approaches" written by Maria del Mar GALOTTO-TÉBAR, Alejandro POMARES-PADILLA, Ivone Alejandra CZERWINSKI y Juan Carlos GUTIERREZ-ESTRADA.

I also attach a copy of the document "Detailed Response to Reviewers" with the response to the editors' and reviewers' comments.

Sincerely,

Ms. Maria del Mar Galotto-Tébar

A handwritten signature in black ink, appearing to be 'M. Galotto', written over the printed name.

**Highlights:**

- European fishing ships are controlled by a vessel monitoring system (VMS).
- FAMI system exceeds in reliability and accuracy the current VMS
- The mobile' sensors can be used by learning machines to predict fishing events.
- Multilayer perceptrons identified correctly 96.26% of the fishing events.

**Table 1.** Sensors used: main characteristics, data generation interval of each sensor (sampling period) and variables extracted from each sensor)

Sensor	Range	Sensitivity	Sampling period	Variable
Acceleration	$\pm 19.6133\text{ m/s}^2$	$0,009570\text{ m/s}^2$	50 ms	AceX AceY AceZ
Gyroscope	$\pm 8.7266\text{ rad/s}$	$0.0002661\text{ rad/s}$	50 ms	GirX GirY GirZ
Magnetometer	$\pm 4900\text{ }\mu T$	$0.6\text{ }\mu T$	50 ms	MagX MagY MagZ
GPS	-	-	1 s	GpsR GpsV



**Table 2.** *Accuracy, precision, recall and F1 score* (expressed as percentages) in the final test of the LDA, MLP, PNN and SVM learning machines. This analysis included the samples recorded during all categories of activity with all their attributes.

Activity	<i>Accuracy</i>	<i>Precision</i>	<i>Recall</i>	<i>F1 Score</i>
<i>LDA</i>				
Steaming	73.63	47.66	55.73	51.38
Setting	77.82	61.07	31.11	41.22
Towing	80.30	62.76	52.14	56.96
Hauling	78.76	55.05	82.05	65.89
<i>MLP</i>				
Steaming	72.15	46.96	70.17	55.93
Setting	80.00	73.00	32.43	43.66
Towing	87.24	71.46	81.97	76.26
Hauling	87.60	78.66	69.42	73.51
<i>PNN</i>				
Steaming	76.88	54.26	47.86	50.86
Setting	71.88	37.10	17.95	24.19
Towing	68.08	40.24	57.09	47.21
Hauling	71.45	44.16	53.68	48.46
<i>SVM</i>				
Steaming	83.80	99.05	35.56	52.33
Setting	86.45	76.69	65.81	70.84
Towing	68.59	44.20	97.61	60.84
Hauling	84.83	84.23	48.38	61.45

**Table 3.** *F1 score* (expressed as a percentage) in the final test of the LDA, MLP, PNN and SVM learning machines. The samples are included with all their attributes. *1-vs-1* includes samples from two categories. *1-vs-Rest* includes all the samples, maintaining the category on the left and grouping the other categories in the *Rest* category.

Type of partition	LDA		MLP		PNN		SVM	
1-vs-1								
Steaming-vs-Setting	59.37	35.58	69.48	44.82	34.46	68.11	57.65	73.77
Steaming-vs-Towing	74.34	77.12	84.94	85.04	51.52	75.39	63.56	78.87
Steaming-vs-Hauling	79.77	84.01	85.12	86.42	58.25	76.27	66.59	79.97
Setting-vs-Towing	90.66	91.05	92.49	91.84	25.89	70.14	87.24	88.58
Setting-vs-Hauling	95.21	95.22	94.14	94.47	81.59	83.44	93.81	93.17
Towing-vs-Hauling	81.23	80.28	66.37	75.58	75.88	54.79	84.83	79.27
1-vs-Rest								
Steaming-vs-Rest	69.43	63.15	75.85	67.77	48.51	73.05	61.26	71.79
Setting-vs-Rest	46.09	65.88	53.16	72.90	73.12	60.32	62.08	69.30
Towing-vs-Rest	60.54	61.67	88.72	88.54	69.60	22.46	71.03	34.95
Hauling-vs-Rest	80.09	70.55	81.84	79.71	74.73	64.62	77.48	61.32

**Table 4.** *F1 score* (expressed as a percentage) for the towing category in the final test of the LDA, MLP, PNN and SVM learning machines with all the attributes and after reducing the number of categories. The results without a reduction and with 3 and 2 categories. The symbol “>” written between two categories indicates that the category on the left is merged with that on the right, the label of the samples of the category on the left being changed to that of the one on the right.

Activity	LDA	MLP	PNN	SVM
<i>Steaming-Setting-Towing-Hauling</i>				
Unreduced	56.96	76.26	47.21	60.84
<i>Steaming-Towing-Hauling</i>				
Setting > Steaming	57.14	73.77	55.70	64.81
Setting > Towing	55.16	68.13	58.70	67.06
<i>Steaming-Setting-Towing</i>				
Hauling > Steaming	41.64	71.15	55.06	18.88
Hauling > Towing	77.75	84.48	64.95	71.16
<i>Steaming-Towing</i>				
Setting > Steaming / Hauling > Steaming	55.47	77.51	70.72	71.05
Setting > Steaming / Hauling > Towing	85.38	87.34	76.18	79.42
Setting > Towing / Hauling > Steaming	44.98	73.97	69.41	53.75
Setting > Towing / Hauling > Towing	76.42	77.81	76.02	79.35

**Table 5.** *Accuracy, precision, recall and F1 score* (expressed as percentages) for the towing category in the final tests of the LDA, MLP, PNN and SVM learning machines, with all the categories and after reducing attributes grouped by sensors. The results are shown before reduction (Ace-Gry-Mag-GPS) and after reduction using the set of sensors that provided the best *F1 score* for the *Towing* phase. The attributes were grouped by sensors as follows: Ace = (AceXm, AceXs, AceYm, AceYs, AceZm, AceZs), Gir = (GirXm, GirXs, GirYm, GirYs, GirZm, GirZs), Mag = (MagXm, MagXs, MagYm, MagYs, MagZm, MagZs) and Gps = (GpsRm, GpsRs, GpsVm, GpsVs).

Sensors	Accuracy	Precision	Recall	F1 Score
<i>LDA</i>				
Ace-Gir-Mag-Gps	80.30	62.76	52.14	56.96
Ace-Gir-Gps	82.35	60.29	86.15	70.94
<i>MLP</i>				
Ace-Gir-Mag-Gps	87.24	71.46	81.97	76.26
Gir-Gps	88.62	74.39	83.37	78.57
<i>PNN</i>				
Ace-Gir-Mag-Gps	68.08	40.24	57.09	47.21
Gps	66.67	42.55	95.21	58.82
<i>SVM</i>				
Ace-Gir-Mag-Gps	68.59	44.20	97.61	60.84
-	-	-	-	-

**Table 6.** *Accuracy, precision, recall, F1 score and Kappa index for the towing category in the final test of the LDA, MPL, PNN and SVM learning machines. The results are shown before reduction (all activities/all sensors) and after the reduction in categories and attributes grouped by sensors that provide the best F1 scores in the towing phase.*

Activities/Sensors	Accuracy	Precision	Recall	F1 Score	Kappa
<i>LDA</i>					
All activities / All sensors	80.30	62.76	52.14	56.96	0.60
Steaming-Towing / Ace-Gir-Gps	84.02	76.78	97.52	85.92	0.73
<i>MLP</i>					
All activities / All sensors	87.24	71.46	81.97	76.26	0.70
Steaming-Towing / Gir-Gps	89.69	85.11	96.26	90.33	0.83
<i>PNN</i>					
All activities / All sensors	68.08	40.24	57.09	47.21	0.34
Steaming-Towing / Gps	74.19	66.45	97.69	79.10	0.54
<i>SVM</i>					
All activities / All sensors	68.59	44.20	97.61	60.84	0.56
Steaming-Towing / All sensors	70.04	62.66	99.23	76.81	0.52



Figure 1



FIGURE 1

Figure 2

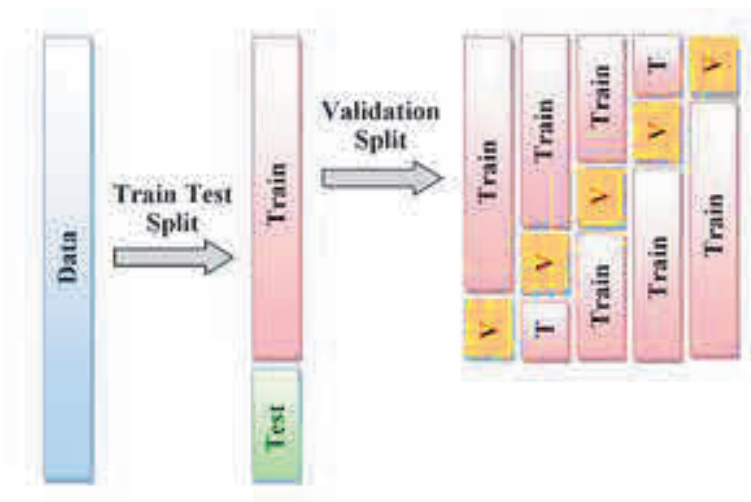


FIGURE 2

Figure 3

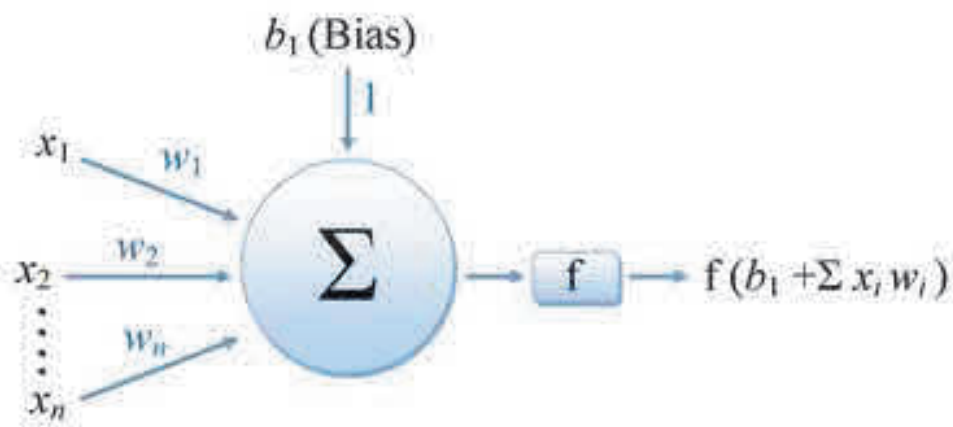


FIGURE 3

Figure 4

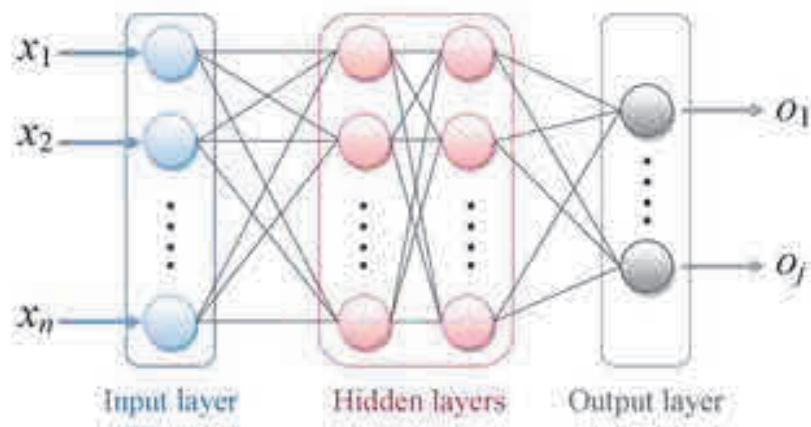


FIGURE 4

Figure 5

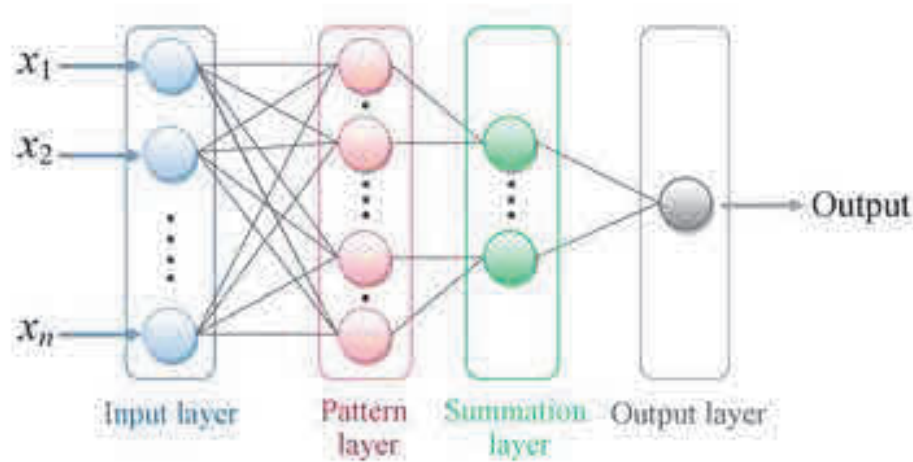


FIGURE 5



Figure 6

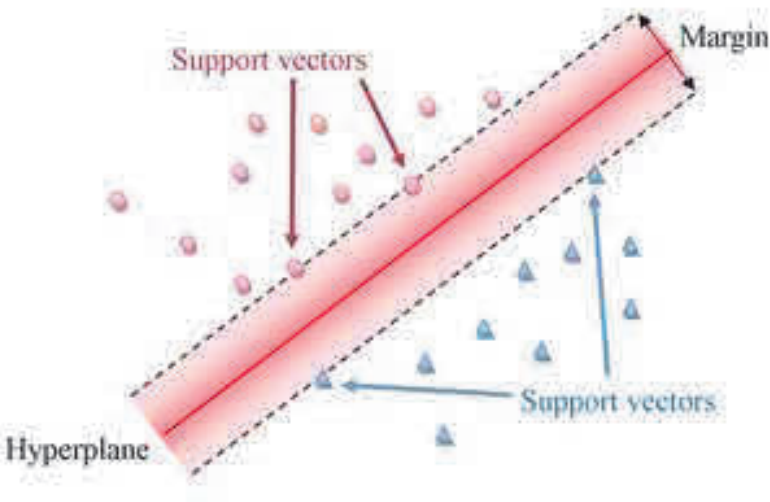


FIGURE 6

## Figure Captions

**Figure 1.** FAMIS user interface installed in a smart phone and information flow.

**Figure 2.** K-fold cross-validation process. The samples from the table of data (Data) are split into training data (Train - T) to be used in the cross-validation process and test data (Test) to be used in the final model assessment. The 5-fold cross-validation process calculates the mean of the results from repeating the model training and validation process five times. Each process uses different data, ensuring that all the data have been used once in the validation phase.

**Figure 3.** Artificial neuron. It sums the inputs ( $x_i$ ) multiplied by the weight associated with each one ( $w_i$ ), adds the bias ( $b$ ) and applies the activation function ( $f$ ).

**Figure 4.** Architecture of the multi-layer perceptron neural network. Input layer with  $n$  neurons that receive input attributes ( $x_n$ ). Hidden layers composed of a variable number of layers and neurons. Output layer that provides the response of the neural network ( $o_j$ ). The lines represent the connections that transmit the data between layers.

**Figure 5.** Architecture of the probabilistic neural network. Input layer with  $n$  neurons that receive input attributes ( $x_n$ ). Pattern layer with one neuron per sample. Summation layer with one neuron per class. Output layer with one neuron providing the output of the neural network.

**Figure 6.** Graphical representation of the hyperplane used by the support vector machine to discriminate samples of different classes. Support vectors show which samples are closest to the hyperplane and define the edge of the margin.

**Figure 7.** Graphical representation of the prediction of 4 hauls of the LDA, MLP, PNN and SVM models. The orange area represents the real hauls, the blue dots the *steaming* prediction and the red dots the *towing* prediction.

Figure 7

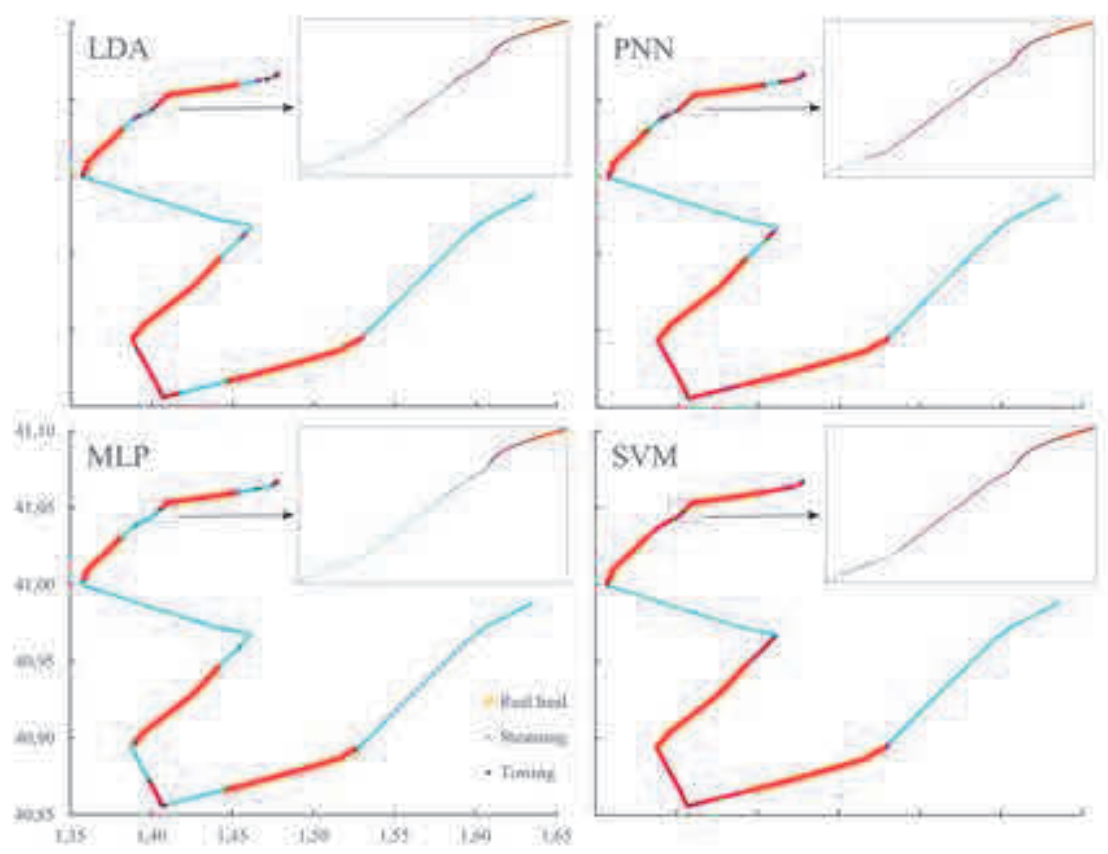


Figure 7

# Maria del Mar Galotto Tébar

<https://orcid.org/0000-0001-6045-4563>

---

**No public information available.**

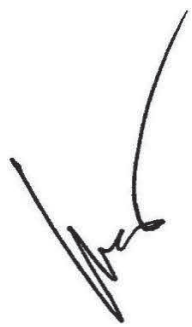
*Record last modified Mar 25, 2021 8:58:28 PM*

## **Credit Author Statement**

**Galotto-Tebar, M.M.:** Conceptualization, Methodology, Software, Validation, Formal analysis, Investigation, Resources, Data Curation, Writing - Original Draft, Visualization; **Pomares-Padilla, A.:** Conceptualization, Methodology, Software, Validation, Formal analysis, Investigation, Resources, Data Curation, Writing - Review & Editing, Visualization; **Czerwinski, I.A.:** Conceptualization, Methodology, Formal analysis, Investigation, Resources, Writing - Review & Editing, Visualization, Supervision; **Gutiérrez-Estrada, J.C.:** Conceptualization, Methodology, Formal analysis, Investigation, Resources, Writing - Review & Editing, Visualization, Supervision

**Declaration of interests**

- ☒ The authors declare that they have no known competing financial interests or personal relationships that could have appeared to influence the work reported in this paper.
- ☐ The authors declare the following financial interests/personal relationships which may be considered as potential competing interests:

A handwritten signature in black ink, consisting of a series of loops and a long, sweeping upward stroke.

# Is the vessel fishing? Discrimination of fishing activity with low-cost intelligent mobile devices through traditional and heuristic approaches

Galotto-Tebar, M.M.<sup>1</sup>; Pomares-Padilla, A.<sup>1</sup>; Czerwinski, I.A.<sup>2</sup>; Gutiérrez-Estrada, J.C.<sup>3</sup>

<sup>1</sup>Dpto. de Ingeniería de Computadores, Universidad Miguel Hernández. Campus de Elche, Avenida del ferrocarril s/n, 03202 Elche, Alicante, Spain (m.galotto@umh.es; pomares@umh.es)

<sup>2</sup>Instituto Español de Oceanografía, Centro Oceanográfico de Cádiz, Puerto Pesquero, Muelle de Levante, s/n, 11006 Cádiz, Spain (ivone.czerwinski@ieo.es)

<sup>3</sup>Dpto. de Ciencias Agroforestales, Escuela Técnica Superior de Ingeniería, Campus de El Carmen, Universidad de Huelva, 21007 Huelva, Spain (juanc@uhu.es)

## Abstract

Knowing the activity of fishing vessels accurately and in real time means a leap in quality in the management of fishing activity. This paper presents the development of a new fishing activity monitoring integral system (FAMIS) that can complement and overcome the limitations of current fishing vessel monitoring systems (VMS). FAMIS is developed on the basis of a low-cost mobile device with GPS sensors, accelerometer, gyroscope and magnetic field and integrates different statistical methods (discriminant functions) and heuristics (artificial neural networks and vectorial support machines) as techniques to classify the information recorded by the sensors of a mobile device during fishing activity. The results obtained with FAMIS indicate that, in general, heuristics have a high degree of discrimination of each of the phases of fishing operation and that, in particular, multilayer perceptrons (MLPs) are capable of correctly identifying 96.3% of towing phases using only GPS and gyro sensors.

## Keywords

Vessel monitoring system; mobile device; sensor; trawl fishing; ship's behavior; machine learning

## 1. Introduction



For the exploitation of living aquatic resources to be sustainable, there is a need to limit the impact of fishing fleets on marine ecosystems. To assess the impact of a fishing vessel during its activity, we use the concept of fishing effort defined as fishing capacity multiplied by the duration of fishing activity (EC, 2007). Fishing capacity can be quantified from the vessel's technical characteristics and the fishing gear used. On the other hand, assessment of the duration of fishing activity requires knowledge of the time during which the fishing capacity of a vessel is effectively operated, a parameter which is highly variable and specific to each type of fisheries and fishing operation. Therefore, to reliably identify the duration of activity of a vessel, we need to have information, beyond just the time spent at sea, that allow us to track the activity of a fishing vessel.

In 1995, the European Commission undertook a pilot project to assess the functionality and costs of various satellite systems that might make it possible to continuously track the position and activity of fishing vessels. The result of this pilot was the implementation, in 2000, of a Vessel Monitoring System (VMS) with the goal of improving the management and monitoring of fishing activity. Specifically, all fishing vessels  $\geq 24$  m long were required to use the VMS, this requirement being extended to vessels  $\geq 15$  m in 2003 and those  $\geq 12$  m in 2012 (EC, 2009). Data provided by the VMS (the vessel's geographical position, course and speed) are transmitted every hour to the Spanish Fisheries Monitoring Centre where all this information is stored and shared internationally in real time with parties in whose waters European vessels operate.

Based on the information provided by the VMS, several authors have proposed actions and protocols to strengthen the monitoring and planning of fishing activity (Gerritsen and Lordan, 2011; Gerritsen et al., 2012; Jennings and Lee, 2012), a large proportion of published studies having focused on estimating fishing effort (Rijnsdorp et al, 1998; Deng et al., 2005; Murawski et al., 2005; Salthaug and Johannessen, 2006; Walter et al., 2007; Fock, 2008; Hintzen and Brunel, 2008). Nonetheless, despite the large amount of information provided by the VMS and the indisputable advantages of its analysis for monitoring the fishing fleet, the long sampling period, the limited information provided in each sample and the exclusion of the coastal fleet limit the reliability and accuracy of the estimations that can be obtained from this information (Russo et al, 2016).

To overcome these limitations, there is a need for new devices and/or monitoring procedures. For example, the Location and Track System for Andalusian Fishing Vessels (SLSEPA), also known as the “green box” system (Junta de Andalucía, 2004) developed by the regional government of Andalusia (Spain) uses the GPRS mobile network to transmit data on location, course and speed of the artisanal fisheries to a control centre at 3-min intervals. The higher sampling rate improves the accuracy of the estimation of fishing effort and spatial distribution of the fleet and the low data transmission costs make the system feasible and operative for vessels <12 m long of the artisanal fleets (Cojan and Burgos, 2015). Despite SLSEPA representing a significant improvement, however, this type of system still relies on assigning the type of activity based on the recorded speed alone (Lee et al., 2010; Burgos et al., 2013).

We intend to develop a new fisheries monitoring system that will provide better quality information and at a low cost to facilitate their deployment across the entire fishing fleet. Considering that fishing gear in operation has an effect on the dynamic behaviour of a vessel (Sun et al., 2011; Russo et al., 2011) and that the manoeuvres of a vessel may be related to its fishing activity, a device equipped with positioning and movement sensors could potentially provide the information necessary to accurately determine when a vessel is fishing.

Previous research has found that the sensors that are usually used in smart mobile devices such as mobile phones and tablets (GPS, accelerometer, gyroscope and compass) are capable of accurately detecting likely changes in the dynamic behaviour of a vessel during each trawl phase (Galotto-Tebar et al., 2020). On the other hand, the processing capacity of these devices enables us to include machine learning algorithms (artificial intelligence) that are able to learn about the dynamic behaviour of a vessel during the different phases of operation and identify the activity of a fishing vessel in real time, at any time.

Along these lines, some authors have succeeded in using various learning machines to classify a situation or recognise movements of objects or people based on data provided by movement sensors from smart mobile devices (Rodríguez-Martín et al., 2013; Tian et al., 2019; Cust et al., 2019). In this paper we have selected four supervised machine learning classification techniques: linear discriminant analysis (LDA) used to classify linearly separable samples, multilayer perceptron (MLP) and support vector machine

(SVM) used to classify non-linearly separable samples and Bayesian classifier or probabilistic neural network (PNN). The selected classifiers are commonly used in various fields such as livestock (Rodero et al., 2012), fisheries (Bertrand et al., 2008; Czerwinski et al., 2007; Gutiérrez-Estrada et al., 2000, 2007, 2008, 2010; Queirolo et al., 2012; Robotham et al., 2010), hydraulic management (Pulido-Calvo and Portela, 2007), economics (Pérez-Ramírez and Fernández-Castaño, 2007), quality control (Gutierrez and Vázquez, 2013), etc.

Given this, the aims of this study were first to assess the viability of a range of statistical and heuristic methods as tools to classify the data retrieved by sensors on a mobile device during fishing activity, and secondly, to test their ability to identify which trawl phase a fishing vessel is in at a given time.

## **2. Material and Methods**

The models developed in this paper works with the Fishing Activity Monitoring Integral System (FAMIS) (Galotto-Tebar et al., 2020). FAMIS is a mobile application (APP) developed with Android Studio that records the vessel's movement during its fishing activity. During the recording, the data provide by the sensors of devices like smart phones and tablets are temporarily stored in a local database (SQLite) linked the fishing phase, ship's informations and fishing gear. When the mobile device connects to a server, it sends the information to a MySQL database. The server allows access to information through the REST API service which allows to analyse the data using RStudio application (Figure 1).

### *2.1. Mobile device and sensors*

In this study, we used a Samsung SM-P600 tablet with movement sensors that include as standard: 6-axis inertial measurement unit (Bosch Sensortec BMI055) composed of a digital triaxial 12-bit acceleration sensor and a digital triaxial 16-bit gyroscope, a 16-bit 3-axis magnetometer (Asahi Kasei Microdevices AK8963C) and a GPS receptor. Using these sensors and sampling periods of 50 ms and 1 s, data were collected on 11 different variables (Table 1).

With the acceleration sensor, we measured the acceleration ( $\overrightarrow{Ace}$ ) of the mobile device while it is moving, this movement being produced when there are external forces on the device, the value recorded being the force acting on the mass of the sensor. Once the mobile device is attached to the vessel's structure, we can say that the movement of the device reflects that of the vessel. One of the forces always involved in the movement and hence in the acceleration recorded by the sensor is gravity (G) (Equation 1). In this equation, the mass is the sum of the mass of the device and that of the vessel; this term can be ignored and we can consider that the accelerometer will record the components of the gravity vector ( $\vec{G}$ ) at each point.

$$\overrightarrow{Ace} = -\vec{G} - \overrightarrow{\Sigma F} / Mass \approx -\vec{G} \quad (1)$$

With the gyroscope sensor, we measure the speed of rotation around the three main coordinate axes: OX, OY and OZ in radians per second (rad/s). If an observer placed on the positive side of an axis detects that the rotation around the axis is anticlockwise, the speed of rotation will be positive and when the rotation is clockwise, the speed of rotation will be negative.

With the magnetometer, we measure the Earth's magnetic field and the magnetic field around the device, in microTesla ( $\mu T$ ). This sensor obtains the vector sum of the Earth's magnetic field and the magnetic fields generated by objects around the device such as engines, cables, etc., and provides the vector components resulting from the sum along OX, OY and OZ axes (Equation 2):

$$\overrightarrow{Mag} = \overrightarrow{Mag_{Earth}} + \overrightarrow{Mag_{Environ}} \quad (2)$$

Using a network of satellites, the global positioning system sensor measures the 3-D geographical position of the device, providing values for latitude, longitude and altitude. The sensor also records the timepoint of the measurement and is able to process these data and generate new information indicating the course, instantaneous and mean velocity, and accuracy. For this study, we have only considered it relevant to record the course (GpsR) and instantaneous speed (GpsV) every second during the activity of the vessel.

## 2.2. Data collection

Data were collected from the fishing and oceanographic research vessel Miguel Oliver of the Spanish General Secretariat for Fisheries, between 28 May and 1 June 1, 2016 in the waters off Castellón, Tarragona, Barcelona and Girona, during the Mediterranean International Trawl Survey (MEDITS)-Spain bottom trawl survey. This survey is undertaken annually by the Spanish National Institute of Oceanography (IEO), to assess demersal fish stock along the continental shelf and slope in the Spanish Mediterranean Sea (Bertrand et al., 2002).

Seeking to record the position of a vessel as accurately as possible, the mobile device was placed in the navigation bridge at around 18 m above the centre of gravity of the boat at the point where the pitch and roll axes intersect (Ibrahim and Grace, 2010), aligning the device with the OY axis parallel to the longitudinal axis (running from stern to prow), the OX axis parallel to the transverse axis (running from port to starboard) and the OZ axis parallel to the vertical axis. The vector information from the sensors is recorded with respect to these coordinate axes. In relation to this, we previously developed a mobile application (FAMIS) to allow users to activate sensors, select a vessel's phase of hauling at each point in time and store the information recorded in a database (Galotto et al., 2020).

We recorded the vessel's movements during 22 trawl hauls using a GOC 73 sampling gear with Morgère trawl doors at a speed of 3 knots, of which 20 were 30-minute hauls at depths of 50 to 200 m and 2 were 60-minute hauls at depths greater than 200 m. We divided the vessel's fishing activity into four phases: steaming, setting, towing and hauling, and recorded the start and end time of each phase of operation.

## 2.3. Automated learning techniques

Automated machine learning refers to a set of techniques that allow computer systems themselves to create algorithms that are able to analyse data and acquire the knowledge necessary to carry out tasks such as predicting, classifying, ranking and decision making, without the need for defining initial rules to facilitate these tasks. For this study, we

selected four supervised automated learning classification techniques with very different strategies: (i) linear discriminant analysis (LDA), a statistical technique that classifies samples that are linearly separable and estimates the probability of being in each group; (ii) support vector machines (SVMs) that classify nonlinearly separable samples using a geometric approach; (iii) multilayer perceptrons (MLPs) that are universal proxies of nonlinear functions; and (iv) Bayesian classifiers or probabilistic neural networks (PNNs).

#### 2.4. Data processing

The first step in data processing was filtering, to eliminate zeros and outliers in the data recorded by the sensors. Next, we created 22 independent continuous quantitative variables (attributes) with a mean ( $X_m$ ) and standard deviation ( $X_s$ ) of the data in 10-s periods, allowing sufficient time for the boat to complete half a pitch/roll cycle (Barras and Derrett, 2012): For the Accelerometer, the mean and standard deviation were recorded for the three axes, resulting in variables  $AceX_m$ ,  $AceX_s$ ,  $AceY_m$ ,  $AceY_s$ ,  $AceZ_m$ , and  $AceZ_s$ . Similar variables were recorded for the gyroscope ( $GirX_m$ ,  $GirX_s$ ,  $GirY_m$ ,  $GirY_s$ ,  $GirZ_m$ ,  $GirZ_s$ ) and the Magnetometer ( $MagX_m$ ,  $MagX_s$ ,  $MagY_m$ ,  $MagY_s$ ,  $MagZ_m$ ,  $MagZ_s$ ). For the GPS the mean and standard deviation for the course and instantaneous speed were recorded:  $GpsR_m$ ,  $GpsR_s$ ,  $GpsV_m$  and  $GpsV_s$ .

We then created an independent nominal qualitative variable (label) called Activity to identify the launch phase of each sample from the official MEDITS-2016 survey data. The labelling of this variable follows a window-type criterion similar to that used by O'Farrell with VMS samples (O'Farrell et al, 2017), assigning the most repeated value during the 10 seconds prior to the sample.

The table of labelled data was created by merging the 22 attributes and the label, removing the records with at least one null, normalising attributes and balancing the samples by activity. As a result, we obtained a total of 6184 samples (1546 samples per activity).

To evaluate the classification performance of each model, we divided the table of data into two blocks: a training data set consisting of 3844 samples (62.16%) from the first 3 days of the survey, covering a total of 15 hauls, and a test data set consisting of 2340

samples (37.83%) from the last 2 days of the survey, during which 7 hauls were completed. This procedure allows models to be trained and tested under different weather conditions.

## 2.5. Assessment metrics

The classification performance of each model is related to the number of hits and misses. In this study, we used five specific metrics to assess the predictive power of the classifiers:

*Accuracy*: Percentage of positive and negative predictions that are correct

$$Accuracy = \frac{(TP+TN)}{(TP+TN+FP+FN)} \times 100 \quad (3)$$

*Precision*: Percentage of positive predictions that are correct

$$Precision = \frac{TP}{(TP+FP)} \times 100 \quad (4)$$

*Recall*: Percentage of true positives retrieved

$$Recall = \frac{TP}{(TP+FN)} \times 100 \quad (5)$$

*F1 Score*: Harmonic mean of precision and recall

$$F1\ Score = \frac{2*Precision*Recall}{(Precision+Recall)} \quad (6)$$

where *TP* stands for *True Positive*, the number of fishing sets correctly predicted to be a member of a class, *TN* for *True Negative*, the number of fishing sets correctly predicted to not be a member of a class, *FP* for *False Positive*, the number of fishing set incorrectly predicted to be a member of a class, and *FN* for *False negative*, the number of fishing sets incorrectly predicted to not be a member of a class.



*Kappa index*: Measure of the degree of agreement between the classifier's prediction and the true classification (Cohen, 1960)

$$Kappa = \frac{p_o - p_e}{1 - p_e} \quad (7)$$

where  $p_o$  is the probability of success of the classifier and  $p_e$  is the probability of success of a random classifier.

## 2.6. Model hyperparameter tuning

Automated learning models are parameterised in order that their behaviour can be adjusted to fit a given problem. These models can have multiple parameters and finding the optimal combination of values sometimes requires in-depth analysis that is beyond the scope of this paper. In this study, we selected the values for each parameter using a grid search procedure for hyperparameters, establishing a discrete range of values for each parameter and creating a grid with all the possible combinations of hyperparameters to methodically assess all the resulting models. The best model was selected based on using the F1 score to compare the model's performance.

To avoid choosing hyperparameters of the model that best fit the test data set, the validation process uses different data to train and validate each configuration, saving the test data set for the final assessment of the model. The validation of each configuration of the model was carried out using k-fold cross-validation resampling (Burman, 1989) (Figure 2). To avoid overly small data sets, we used  $K=5$ . Having selected the parameters that provided the best results in the validation process, the model was trained with all the training data and then the classification performance is assessed with the test data.

## 2.7. Simplification of the model

The samples recorded during the vessel's fishing activity reflect the influence of trawling on the dynamic behaviour of the vessel. Galotto et al. (2020) demonstrated that the sensors of a mobile device were capable of identifying four distinct periods labelled: steaming, setting, towing and hauling. The task of the models used in this study is to classify the samples into one of these four categories. We should recall that the main

objective of this study is to identify the start and end of trawling to obtain real-time information on fishing, and hence, the efficacy in recognising the samples taken during the towing phase is key to achieving this objective. The remaining phases could potentially be merged, thereby reducing the number of phases, if, by doing so, we improve the performance of the model when classifying the towing category. In relation to this, we validated the models with 4, 3, and 2 categories, always keeping the towing category.

The inclusion of too many attributes of samples may lead to learning machines performing the classification task less well. Given that each attribute is linked to a sensor, and in some cases, to the orientation of the mobile device with respect to the vessel, we grouped the attributes by sensor, and analysed the response of the four learning machines to all of the potential reductions in the group of attributes.

## *2.8. Machine learning*

### *2.8.1. Linear discriminant analysis (LDA)*

Linear discriminant analysis (LDA) is a supervised learning algorithm used for data classification and dimension reduction. Based on a dependent qualitative variable and a set of independent quantitative variables, discriminant analysis allows samples to be classified into one of the groups established by the dependent variable.

This type of analysis provides classification procedures for new observations with an unknown origin into one of the groups analysed, by providing discriminant scores from which we can estimate the probability of being in each group. For this, the algorithm uses new variables known as discriminant variables that are able to characterise and differentiate between groups, described using discriminant functions which are linear combinations of the original variables. More detailed descriptions of the method can be found in Kim et al. (2007), Berstein et al. (2019) and Li et al. (2020).

### *2.8.2. Artificial neural networks: multilayer perceptrons (MLPs) and probabilistic neural networks (PNNs)*

Artificial neural networks are mathematical models inspired by the neural architecture of the human brain (Rumelhart et al, 1986). To create an artificial neural system, we use

artificial neurons functionally organised in layers. The information flows through the layers of the neural network via one-way connections that simulate the synapses between neurons. Each connection has an associated weight ( $w_i$ ) equivalent to the synapse strength, and each input ( $x_i$ ) through this connection is multiplied by this weight. The receptor neurone calculates the weighted sum of all the inputs, adds a numerical value known as bias ( $b$ ) and applies an activation function to the result ( $f$ ) to determine the output (Figure 3).

In particular, multilayer perceptrons (MLPs) are one-way neural networks formed by an input layer with as many neurons as there are input attributes, one or several hidden layers with a variable number of neurons and output layer with the number of neurons required to show the output (Figure 4). The data flow in one direction from the input layer towards the output layer. The outputs from each neuron of the input layer and hidden layers are connected to the input neurons of the following layer. MLPs are able to analyse complex data sets and perform nonlinear classification into two or more groups, and given this, have been widely used in a range of technical applications (Lek and Guegan, 1999; Gutiérrez-Estrada et al., 2000; Dedeker et al., 2005; Goethals et al., 2007; Pulido-Calvo and Portela, 2007; Gutiérrez-Estrada et al., 2008).

On the other hand, probabilistic neural networks (PNNs) are Bayes-Parzen classifiers composed of four layers: an input layer with the same number of neurons as input attributes; a first hidden layer, which is a pattern layer with the same number of neurons as training or calibration samples; a second hidden layer, which is a summation layer with the same number of neurons as classes; and an output layer, with a neuron that provides the result of the classification (Figure 5) (Specht and Specht, 1990; Hajmeer and Basheer, 2002; Rodero et al., 2012).

When we supply an input to the PNN, the pattern layer assesses the distances from the input vector to the training vectors using a vector of distances, the elements of which indicate how close the input is to each training input. The summation layer (the second layer) sums the patterns of each class generating a vector of probabilities which is then used by a competitive transfer function at the output layer to select the most probable class (Pérez-Ramírez and Fernando-Castaño, 2007).

### 2.8.3. Support Vector Machine

The support vector machine (SVM) are statistical classifiers proposed by Vapnik (1995) that belong to a family of linear classifiers. SVMs seek to identify hyperplanes that divide the input feature space. At the algorithmic level, SVM learning is modelled as a quadratic optimisation problem with linear constraints, the size of the problem depending on the dimension of the feature space (Figure 6). While markedly less popular than the aforementioned models, they have been used in a range of applications and shown a discriminatory power similar to that of MLPs (Robotham et al., 2010; Rodero et al., 2012).

### 2.9. Calibration and validation procedures

The construction of learning machine models starts with the processes of validation (k-fold cross-validation) and parameter section allowing adaption of their behaviour to the problem to be solved. In the case of the LDA modelling, given the use of balanced samples, the initial probability of class membership is the same for all the classes. In MLP modelling, the following were selected: a hidden layer with 8 neurons, a maximum of 30 iterations of learning, `Randomize_Weights(0,1)` as the initialization function, `Std_Backpropagation(0.2,0)` as the learning function, `Topological_Order(0)` as the update function, and `Act_Logistic` as the activation function of all hidden units and all output units. As the initialisation function assigns random initial weights, producing small differences between the models, we calculated the mean of 10 training and testing runs of the MLP. In the PNN modelling, a value of 1.4 was set as the smoothing parameter for the pattern-layer activation function. Lastly, in the SVM modelling, we chose a linear kernel and set the constraint violation cost to 1.

For data processing, simulating the learning machines and obtaining the results, we used the R programming language (<https://www.r-project.org>) with specific libraries to work with learning machines such as Modern Applied Statistics with S (Ripley et al., 2020), R Neural Networks using the Stuttgart Neural Network Simulator (<https://github.com/cbergmeir/RSNNS>), probabilistic neural networks PNN (Chasset, 2016) and Misc Functions of the Department of Statistics Probability Theory Group (E1071; Meyer, 2019).

### 3. Results

Table 2 shows the results concerning the performance in the final test of the four learning machines analysed in this study.

In general, MLPs and SVMs provided better results than LDA or PNNs. The best harmonic mean between precision and recall (F1 scores) was obtained with the SVM model, with a mean among the categories of 68.21% compared to the 65.41% observed in the MLP model. Further, the SVM model was better than the MLP model in precision, with a mean of 76.04% compared to 67.52%. In contrast, the MLP model was better in terms of accuracy and sensitivity, with mean percentages of 81.75% and 63.50% compared to 80.92% and 61.84% in the SVM model. On the other hand, the MLP model provided more balanced results than the SVM one, with regards to classifying the samples recorded during the trawling phase, with an accuracy of 87.24%, a precision of 71.46% and an F1 score value of 76.26%. The SVM model only performed better than the MLP model in terms of sensitivity, being able to identify 97.61% of the trawling activity samples, at the expense of a very high number of false positives. We should highlight the difficulties of the LDA, MLP and PNN models in identifying the setting category, these only being able to recognise 31.11%, 32.43% and 17.95%, respectively, of the samples recorded in this phase.

Table 3 presents the ability of learning machines to distinguish samples from two fishing phases. The analysis from using samples from two trawl phases (1 versus 1) is reported in the top half of the table and from using all the samples, three phases being merged in a new class called “the rest” (1 versus the rest) in the bottom half. This table provides F1 scores as a percentage in the final test of the four models. The results obtained reveal the weaknesses of the LDA, MLP and PNN models in different trawl phases. The LDA and MLP models struggle to differentiate samples from the steaming and setting phases, being able to identify less than 33% of the samples recorded during setting. On the other hand, the PNN model did not differentiate well between steaming and setting, but in this case, the poor results correspond to the steaming phase, this model identifying only 22.56% of the samples obtained during steaming. Similarly, the PNN provided poor results for

differentiating between setting and towing, being able to identify only 14.87% of the samples from the setting phase.

Next, we explored the possibility of improving performance in the classification process by reducing the number of categories, testing all four models, maintaining the towing and steaming activities and removing the setting or hauling categories or both. Table 4 shows that all the models performed better in classifying towing (F1 score) when setting and hauling were eliminated and assigning the samples taken in these phases to steaming and towing, respectively.

We also explored the response of the four models to a reduction in the number of input attributes. For this purpose, we grouped the attributes by sensor and tested all the possible combinations. Table 5 shows the F1 score for towing with each of the four models with all the attributes and the best response to a potential reduction in attributes grouped by sensor. We can observe the substantial improvement in the LDA model after removing the variables based on data from the magnetometer while the PNN model provided better results using only the GPS-based attributes. Similarly, the MLP model improved 3% using only the gyroscope- and GPS-based attributes, while the performance of the SVM model did not improve by reducing attributes.

Table 6 shows the results in the final test of the four models considering the reduction of attributes and categories. The MLP model performs markedly better than the others, with a hit rate of 89.69% in their positive and negative predictions concerning the towing phase, a positive predictive rate of 85.11%, a towing phase sample identification rate of 96.26%, a harmonic mean precision and recall of 90.33%, and a Kappa index with a high degree of agreement of 0.83 ( $p < 0.0001$ ). Figure 6 shows graphically a part of the final test of the models.

#### **4. Discussion**

The information provided by the VMS (position, course and speed) to identify fishing grounds and the activity of a fishing fleet can be improved using additional sensors as is suggested in this study. In trawl fishing, precision is key to assessing haul duration and track, the spatial and time distribution of the effort, and subsequently the catch per unit

effort in each fishing area. Deng (2005) stated that the errors in the prediction of trawl fishing increase with the time interval between VMS records and that the loss in precision is relatively high with sampling intervals longer than 30 minutes. On the other hand, Mills et al. (2007) indicated that a vessel's speed alone is not a suitable criterion for identifying trawling activity and confirmed that the sampling frequency of the VMS is too low to allow trawl tracks to be characterised, most trawls being represented by just one record and some not being detected at all, the haul occurring between two records. In addition, for Peruvian anchoveta, Bertrand et al. (2008) reported that speed provided by VMS data leads to the number of fishing events being overestimated by nearly 182%. These findings warrant the development and deployment of new low-cost monitoring systems, complementary to VMS, that are flexible and easily upgradeable and that allow accurate estimation of the activities of fishing vessels.

Since the deployment of the VMS in 2000, many researchers have studied how to process and complement the data provided by this system to improve the management and monitoring of fishing activity. For example, Szostek et al. (2017) included information extracted from interviews of fishermen about their experience fishing king scallops in the English Channel, while Bastardie et al. (2010) combined the data provided by the VMS with information extracted from logbooks through a linking process considering the degree of mismatch. In these ways, these authors were able to obtain disaggregated fishing effort data at a fine geographical scale. Overall, they indicate that the procedures they used significantly improve the delimitation of the catchment area as well as the assessment of fishing effort in time and space, but to achieve this, there was a need for offline processing of external data and its subsequent integration with data generated by the VMS. In relation to this, the data provided by FAMIS (Galotto et al., 2020), the system we propose, is at the same level as that from VMS, and hence, it is fully complementary and therefore easy to integrate.

The use of the FAMIS in fishing vessels would significantly improve on the use of the VMS alone, as it adds movement sensors on the vessel and processing capacity to allow the use of artificial intelligence algorithms to identify the activity of a vessel in situ. Galotto et al. (2020) showed that standard low-cost devices such as mobile phones and tablets do record different data in each trawl phase, and building on that, in this study, we



demonstrate that certain models, such as MLPs or SVMs, yield classifiers that are good tools for automated classification.

The four types of models analysed in this study use very different classification strategies, and in line with that, their classification performance varied. The results obtained with samples recorded in the four trawl phases and attributes associated with the four sensors indicated that SVMs and MLPs provide better results than LDA and PNNs. These results are similar to those obtained by other authors. Robotham et al. (2010) found that MLPs and SVMs performed significantly better than PNNs or LDA, when attempting to distinguish between four pelagic fish species caught off the northern coast of Chile based on echograms of fish shoals. Further, Rodero et al. (2012) compared the same four types of models for distinguishing between four Andalusian cattle breeds based on morphometric variables and found that MLPs and SVMs had better classification performance. This is attributable to the fact that both MLPs and SVMs associate highly nonlinear discriminant functions with the input patterns. This is a result of the large number of variables in each sample, the physical magnitudes that they represent and the complexity of the identification task, in our case, the identification of movement patterns of a vessel exposed to forces from the waves, wind, engine, rudder and fishing gear.

The high nonlinearity of the input data is clearly reflected in the inability of LDAs to find a discriminant function that distinguishes the samples from different classes. In relation to this, the PNN-based model, which takes a radial approach, identifying new samples based on similarities with training samples, provided the poorest results with a mean F1 score of just 44%. In contrast, the MLP as a universal classifier, with a single hidden layer and a small number of neurons, provided an F1 score of 65.41%, being able to identify nearly 82% of samples in the trawl phase. Finally, the most efficient configuration of the SVM model with a linear kernel finds spaces with new dimensions where it is possible to separate different classes with hyperplanes, providing an acceptable mean F1 score of 68.21% and excellent recall of the trawl phase of over 97%.

These results significantly improve on the classification performance found by previous authors based on VMS data. Gerritsen and Lordan (2011) reported that the use of vessel speed as a classification criterion for fishing activity provided a low rate of false negatives but a very high rate of false positives in the classification (32%), only 68% of cases being

correctly classified. These authors highlighted that the potential reasons for these results are related to the fact that a boat may travel at a speed similar to that when trawling when sail at a slow speed while waiting for the right tide or because of poor weather conditions, among other factors.

In relation to this, the four trawl phases identify periods in time when the fishing vessel is involved in different activities. In each phase, the dynamic behaviour of the vessel is influenced by various elements involved such as speed, course, waves, fishing gear, catch, etc. These elements have a different impact at each phase. For example, the steaming phase ends when the boat is manoeuvring and slowing down until it positions itself where it is going to start trawling. After that, the setting phase starts by shooting the net; then the doors are set and the towing cable paid out. During the towing phase, the drag on the vessel grows as the growing volume of the catch is added to the resistance of the fishing gear itself. Next, in the hauling phase, the towing cable is winched in, the doors are raised, and finally, the fishing gear and the catch are brought on board. At the end of the haul, the vessel starts a new steaming phase, manoeuvring and increasing its speed to move to the next fishing spot. Given all this, the effect of the different manoeuvres within each phase on the behaviour of the vessel cannot be detected by the speed data provided by the VMS unless this information is complemented with movement sensor data such as those recorded through FAMIS.

On the one hand, homogenous behaviour of the vessel within a phase and marked changes between phases should facilitate the task of classifying the samples and identifying the start and end of the trawl phases. The start of setting is the most problematic time point. This is because until the doors are in the water, the resistance of the nets is low and the behaviour of the vessel is similar to that in the steaming phase. In contrast, the towing phase starts when the fishing gear, moving at the towing speed, reaches the correct depth, the cable stops being paid out and the speed of the vessel is reduced to the towing speed. This change of speed enables the models to identify the first samples of the towing phase and therefore the start of the real phase of fishing. Similarly, the hauling phase is easy to identify, given that it starts with a reduction in the vessel's speed to make it easier to bring the fishing gear on board and finishes with the fishing gear inactive and an increase in the vessel's speed.

The results of the models analysed are significantly better when we simplify the description of the activity of the fishing vessel to two phases, a common approach for discriminating the activity in a fishing boat when onboard observers log whether the boat is “fishing” or “not fishing” as a function of whether the fishing gear is deployed in the water (Chang and Yuan, 2014).

By merging the phases steaming+setting and towing+hauling, we obtained F1 scores of over 76% in all the models. These proposed mergers avoid the difficulty of identifying the samples at the start of the setting phase and considers that the vessel is fishing from when it starts towing until the fishing gear is taken out of the water. This is partially consistent with the results of Joo et al. (2011) who used MLPs to estimate fishing events in Peruvian anchoveta fisheries, based on VMS parameters and validated in-situ by onboard observers. In that study, observers validated two segments of activity in the speed data series provided by VMS, identified as acceleration between the previous and current pace (which would coincide in part with the merging of steaming+setting) and the acceleration between the current and the following pace (approximately towing+hauling).

In relation to the sensor systems used in this study, we should indicate that all four sensors provided relevant information about changes in the vessel’s behaviour in the four trawl phases (Galotto et al., 2020). The reduction in computational costs associated with removing variables had a relatively small impact on the behaviour of the models. The sensitivity analysis indicated that the GPS sensor is undoubtedly the device that provides the most important information, given that using this device alone, the models assessed achieved a mean F1 score of over 61%. However, the use of information from the other sensors improved the behaviour of some models. For example, the MLP model was able to correctly identify 96.26% of the samples recorded by the GPS+gyroscope in the towing phase. Specifically, for a standard 60-minute haul, the model identified the act of fishing during 57 minutes and 45 seconds, in the worst-case scenario with the false negatives concentrated at the start or end of trawling. The prediction error of 2 minutes and 45 seconds translates to the identification of a shorter-duration hauling operation and an advance or delay in the start or end of the hauling. On the other hand, we should bear in mind that characteristics of the boat where we performed our experiment (Miguel Oliver) mean that it had a higher vessel size to fishing gear ratio than that in fishing boats. This suggests that the dynamics in a fishing boat may be even more affected by the fishing

gear, and hence, the difference between the trawl phases will be easier to identify using this system.

## Conclusions

The results of this work indicate that the use of the proposed device (FAMIS) on the basis of a mobile device with GPS, accelerometer, gyroscope and magnetic field sensors significantly improves the accuracy of current VMS systems.

The 4 models analysed have shown different capacities to classify fishing activity. The results obtained with samples recorded in the 4 phases of the set (steaming, setting, towing and hauling) and attributes associated with the 4 sensors (Gps, accelerometer, gyroscope and magnetic field) indicate that the SVM and MLP models offer better results than the LDA and PNN models.

On the other hand, the reduction to 2 phases (steaming and towing) considering that the towing phase starts when the fishing gear reaches the correct depth and trawling speed, and ends when the fishing gear is on the deck of the vessel, facilitates the task of classification and substantially improves the results of the 4 models. Furthermore, the reduction of the sensors involved in each model also improves the quality of their predictions.

In summary, the results of this work indicate that the proposed system is capable of classifying the information recorded by the sensors of a mobile device during fishing activity and identifying the phase of the set in which the vessel is at any given time.

## References

- Alfaro-Cortés, E. (2006). Combinación de clasificadores mediante el método boosting. Una aplicación a la predicción del fracaso empresarial en España. PhD Thesis, University of Castilla la Mancha (Spain).
- Barrass, C. B., & Derrett, D.R. (2012). Ship Stability for Masters and Mates. Elsevier Ltd.

643 Bastardie, F., Nielsen, J.R., Ulrich, C., Egekvist, J., & Degel, H. (2010). Detailed mapping  
644 of fishing effort and landings by coupling fishing logbooks with satellite-recorded  
645 vessel geo-location. *Fisheries Research*, 106(1), 41-53.

646 Bernstein, R., Osadchy, M., Keren, D., & Schuster, A. (2019). LDA classifier monitoring  
647 in distributed streaming systems. *Journal of Parallel and Distributed Computing*, 123,  
648 156-167.

649 Bertrand, J. A., Gil de Sola, L., Papaconstantinou, C., Relini, G., & Souplet, A. (2002).  
650 The general specifications of the MEDITS surveys. *Scientia Marina*, 66(2), 9-17.

651 Bertrand, S., Díaz, E., & Lengaigne, M. (2008). Patterns in the spatial distribution of  
652 Peruvian anchovy (*Engraulis ringens*) revealed by spatially explicit fishing data.  
653 *Progress in Oceanography*, 79(2-4), 379-389.

654 Burman, P. (1989). A comparative study of ordinary cross-validation, v-fold cross-  
655 validation and the repeated learning-testing methods. *Biometrika*, 76(3), 503-514.

656 Chang, S.K., & Yuan, T.L. (2014). Deriving high-resolution spatiotemporal fishing effort  
657 of large-scale longline fishery from vessel monitoring system (VMS) data and  
658 validated by observer data. *Canadian Journal of Fisheries and Aquatic Sciences*, 71,  
659 1363–1370.

660 Chasset, P.O. (2016). Package pnn. <https://cran.r-project.org/web/packages/pnn/pnn.pdf>.

661 Cohen, J. (1960). A Coefficient of Agreement for Nominal Scales. *Educational and*  
662 *Psychological Measurement*, 20, 1.

663 Cojan, M., & Burgos, C. (2015). Análisis de la información proporcionada por los  
664 sistemas de localización vía satélite de la flota que explota la chirila (*Chamelea gallina*)  
665 en el Golfo de Cádiz. In *Teledetección: Humedales y Espacios Protegidos. XVI*  
666 *Congreso de la Asociación Española de Teledetección*, 550-553  
667 <http://ocs.ebd.csic.es/index.php/AET/2015/schedConf/presentations>.

668 Council of the European Union. (2009). Establishing a Community control system for  
669 ensuring compliance with the rules of the common fisheries policy, amending  
670 Regulations. *Official Journal of the European Union*, L343, 1-50.

671 Cust, E. E., Sweeting, A. J., Ball, K., & Robertson, S. (2019). Machine and deep learning  
672 for sport-specific movement recognition: a systematic review of model development  
673 and performance. *Journal of Sports Sciences*, 37(5), 568-600.

674 Czerwinski, I.A., Gutiérrez-Estrada, J.C., & Hernando-Casal, J.A. (2007). Short-term  
675 forecasting of halibut CPUE: Linear and non-linear univariate approaches. *Fisheries*  
676 *Research*, 86(2-3), 120-128.

677 Dabiri, S., Marković, N., Heaslip, K., & Reddy, C.K. (2020). A deep convolutional neural  
678 network based approach for vehicle classification using large-scale GPS trajectory  
679 data. *Transportation Research Part C: Emerging Technologies*, 116, 102644-102644.

680 Deng, R., Dichmont, C., Milton, D., Haywood, M., Vance, D., Hall, N., & Die, D. (2005).  
681 Can vessel monitoring system data also be used to study trawling intensity and  
682 population depletion? The example of Australia's northern prawn fishery. *Canadian*  
683 *Journal of Fisheries and Aquatic Sciences*, 62(3), 611-622.

684 European Commission. (2007). On improving fishing capacity and effort indicators under  
685 the common fisheries policy. [http://eur-lex.europa.eu/legal-](http://eur-lex.europa.eu/legal-content/EN/TXT/PDF/?uri=CELEX:52007DC0039&from=EN)  
686 [content/EN/TXT/PDF/?uri=CELEX:52007DC0039&from=EN](http://eur-lex.europa.eu/legal-content/EN/TXT/PDF/?uri=CELEX:52007DC0039&from=EN).

687 Galotto-Tebar, M.M., Pomares-Padilla, A., Czerwinski, I.A., & Gutiérrez-Estrada, J.C.  
688 (2020). Using mobile device's sensors to identify fishing activity. *Journal of Marine*  
689 *Science and Technology*, 25, 978-989.

690 Gerritsen, H., & Lordan, C. (2011). Integrating vessel monitoring systems (VMS) data  
691 with daily catch data from logbooks to explore the spatial distribution of catch and  
692 effort at high resolution. *ICES Journal of Marine Science*, 68(1), 245-252.

693 Gerritsen, H.D., Lordan, C., Minto, C., & Kraak, S.B.M. (2012). Spatial patterns in the  
694 retained catch composition of Irish demersal otter trawlers: High-resolution fisheries  
695 data as a management tool. *Fisheries Research*, 129-130, 127-136.

696 Gloaguen, P., Woillez, M., Mahévas, S., Vermard, Y., & Rivot, E. (2016). Is speed  
697 through water a better proxy for fishing activities than speed over ground? *Aquatic*  
698 *Living Resources*, 29 (210), 1-8.

699 Global Fishing Watch (2012). <https://globalfishingwatch.org>.

700 Gutierrez, P.T., & Vázquez, J.A., (2013). Aplicación de la red neuronal probabilística  
701 para la clasificación de productos conforme a sus especificaciones. *Innovation in*  
702 *engineering, technology and education for competitiveness and prosperity*, 1-10.

703 Gutiérrez-Estrada, J.C., Pulido-Calvo, I., & Prenda, J. (2000). Gonadosomatic index  
704 estimates of an introduced pumpkinseed (*Lepomis gibbosus*) population in a

705 Mediterranean stream, using computational neural networks. *Aquatic Sciences*, 62(4),  
706 350-363.

707 Gutiérrez-Estrada, J.C., Silva, C., Yáñez, E., Rodríguez, N., & Pulido-Calvo, I. (2007).  
708 Monthly catch forecasting of anchovy (*Engraulis ringens*) in the north area of Chile:  
709 Non-linear univariate approach. *Fisheries Research*, 86(2-3), 188-200.

710 Gutiérrez-Estrada, J. C., Vasconcelos, R., & Costa, M. J. (2008). Estimating fish  
711 community diversity from environmental features in the Tagus estuary (Portugal):  
712 Multiple Linear Regression and Artificial Neural Network approaches. *Journal of*  
713 *Applied Ichthyology*, 24(2), 150-162.

714 Gutiérrez-Estrada, J.C., & Bilton, D. T. (2010). A heuristic approach to predicting water  
715 beetle diversity in temporary and fluctuating waters. *Ecological Modelling*, 221(11),  
716 1451-1462.

717 Hajmeer, M., & Basheer, I. (2002). A probabilistic neural network approach for modeling  
718 and classification of bacterial growth/no-growth data. *Journal of Microbiological*  
719 *Methods*, 51(2), 217-226.

720 Heyn, H.M., Blanke, M., & Skjetne, R. (2019). Ice Condition Assessment Using Onboard  
721 Accelerometers and Statistical Change Detection. *IEEE Journal of Oceanic*  
722 *Engineering*, 1-17.

723 Hintzen, N.T., Bastardie, F., Beare, D., Piet, G.J., Ulrich, C., Deporte, N., Egekvist, J., &  
724 Degel, H. (2012). VMStools: Open-source software for the processing, analysis and  
725 visualisation of fisheries logbook and VMS data. *Fisheries Research*, 115-116, 31-43.

726 Ibrahim, R. A., & Grace, I.M. (2010). Modeling of Ship Roll Dynamics and Its Coupling  
727 with Heave and Pitch. *Mathematical Problems in Engineering*, 2010, 1-32.

728 Ichimura, S., & Zhao, Q. (2019). Route-Based Ship Classification. *IEEE 10th*  
729 *International Conference on Awareness Science and Technology (iCAST)*, 1-6.

730 Jennings, S., & Lee, J. (2012). Defining fishing grounds with vessel monitoring system  
731 data. *ICES Journal of Marine Science*, 69(1), 51-63.

732 Joo, R., Salcedo, O., Gutierrez, M., Fablet, R., & Bertrand, S. (2015). Defining fishing  
733 spatial strategies from VMS data: Insights from the world's largest monospecific  
734 fishery. *Fisheries Research*, 164, 223-230.



735 Junta de Andalucía (2004). Localización y seguimiento de embarcaciones pesqueras  
736 (SLSEPA).<http://www.juntadeandalucia.es/organismos/agriculturapescaydesarrollorural/areas/pesca-acuicultura/slsepa.html>.  
737

738 Kim, H., Drake, B.L., & Park, H. (2007). Multiclass classifiers based on dimension  
739 reduction with generalized LDA. *Pattern Recognition*, 40(11), 2939-2945.

740 Lee, J., South, A.B., & Jennings, S. (2010). Developing reliable, repeatable, and  
741 accessible methods to provide high-resolution estimates of fishing-effort distributions  
742 from vessel monitoring system (VMS) data. *ICES Journal of Marine Science*, 67(6),  
743 1260-1271.

744 Li, C.N., Shao, Y.H., Yin, W., & Liu, M.Z. (2020). Robust and Sparse Linear  
745 Discriminant Analysis via an Alternating Direction Method of Multipliers. *IEEE*  
746 *Transactions on Neural Networks and Learning Systems*, 31(3), 915-926.

747 Marzuki, M.I., Garello, R., Fablet, R., Kerbaol, V., & Gaspar, P. (2015). Fishing gear  
748 recognition from VMS data to identify illegal fishing activities in Indonesia. In  
749 *MTS/IEEE OCEANS 2015 - Genova*, 1-5.

750 Masters, T (1995). Advanced algorithms for neural networks : a C++ sourcebook. Wiley.

751 Meyer, D. (2019). Package e1071. [https://cran.r-](https://cran.r-project.org/web/packages/e1071/e1071.pdf)  
752 [project.org/web/packages/e1071/e1071.pdf](https://cran.r-project.org/web/packages/e1071/e1071.pdf).

753 Mills, C.M., Townsend, S.E., Jennings, S., Eastwood, P.D., & Houghton, C.A. (2007).  
754 Estimating high resolution trawl fishing effort from satellite-based vessel monitoring  
755 system data. *ICES Journal of Marine Science*, 64(2), 248-255.

756 Neural Networks in R using the Stuttgart Neural Network Simulator.  
757 <https://github.com/cbergmeir/RSNNS>.

758 O'Farrell, S., Sanchirico, J. N., Chollett, I., Cockrell, M., Murawski, S. A., Watson, J. T.,  
759 Haynie, A., Strelcheck, A., & Perruso, L. (2017). Improving detection of short-  
760 duration fishing behaviour in vessel tracks by feature engineering of training data.  
761 *ICES Journal of Marine Science*, 74(5), 1428-1436.

762 Palmer, M.C. (2008). Calculation of distance traveled by fishing vessels using GPS  
763 positional data: A theoretical evaluation of the sources of error. *Fisheries Research*,  
764 89(1), 57-64.



765 Pérez-Ramírez, F.O., & Fernández-Castaño, H. (2007). Las redes neuronales y la  
766 evaluación del riesgo de crédito. *Revista Ingenierías Universidad de Medellín*, 6(10),  
767 77-91.

768 Politis, P.J., DeAlteris, J.T., Brown, R.W., & Morrison, A.T. (2012). Effects of sea-state  
769 on the physical performance of a survey bottom trawl. *Fisheries Research*, 123-124,  
770 26-36.

771 Pulido-Calvo, I., & Portela, M.M. (2007). Application of neural approaches to one-step  
772 daily flow forecasting in Portuguese watersheds. *Journal of Hydrology*, 332(1-2), 1-  
773 15.

774 Queirolo, D., Hurtado, C.F., Gaete, E., Soriguer, M.C., Erzini, K., & Gutiérrez-Estrada,  
775 J.C. (2012). Effects of environmental conditions and fishing operations on the  
776 performance of a bottom trawl. *ICES Journal of Marine Science*, 69(2), 293-302.

777 Ripley, B., Venables, B., Bates, D.M, Hornik, K., Gebhardt, A., & Firth, D. (2020).  
778 Package mass. <http://www.stats.ox.ac.uk/pub/MASS4/>.

779 Robotham, H., Bosch, P., Gutiérrez-Estrada, J. C., Castillo, J., & Pulido-Calvo, I. (2010).  
780 Acoustic identification of small pelagic fish species in Chile using support vector  
781 machines and neural networks. *Fisheries Research*, 102(1-2), 115-122.

782 Rodero, E., González, A., Luque, M., Herrera, M., & Gutiérrez-Estrada, J.C. (2012).  
783 Classification of Spanish autochthonous bovine breeds. Morphometric study using  
784 classical and heuristic techniques. *Livestock Science*, 143 (2-3), 226-232.

785 Rodriguez-Martin, D., Samà, A., Perez-Lopez, C., Català, A., Cabestany, J., &  
786 Rodriguez-Molinero, A. (2013). SVM-based posture identification with a single waist-  
787 located triaxial accelerometer. *Expert Systems with Applications*, 40(18), 7203-7211.

788 Rumelhart, D.E., Hinton, G.E., & Williams, R.J. (1986). Learning representations by  
789 backpropagation errors. *Nature*, 323, 533-536.

790 Russo, T., Parisi, A., Prorgi, M., Boccoli, F., Cignini, I., Tordoni, M., & Cataudella, S.  
791 (2011). When behaviour reveals activity: Assigning fishing effort to métiers based on  
792 VMS data using artificial neural networks. *Fisheries Research*, 111, 53-64.

793 Russo, T., D'Andrea, L., Parisi, A., Martinelli, M., Belardinelli, A., Boccoli, F., Cignini,  
794 I., Tordoni, M. & Cataudella, S. (2016). Assessing the fishing footprint using data

795 integrated from different tracking devices: Issues and opportunities. *Ecological*  
796 *Indicators*, 69, 818-827.

797 Shepperson, J., Murray, L.G., Mackinson, S., Bell, E., & Kaiser, M.J. (2016). Use of a  
798 choice-based survey approach to characterise fishing behaviour in a scallop fishery.  
799 *Environmental Modelling & Software*, 86, 116-130.

800 Simeone, O. (2018). A Very Brief Introduction to Machine Learning With Applications  
801 to Communication Systems. *IEEE Transactions on Cognitive Communications and*  
802 *Networking*, 4(4), 648-664.

803 Specht D. F. (1990). Probabilistic Neural Networks. *Neural Networks*, 3, 109-118.

804 Sun, X., Yin, Y., Jin, Y., Zhang, X., & Zhang, X. (2011). The modeling of single-boat,  
805 mid-water trawl systems for fishing simulation. *Fisheries Research*, 109(1), 7-15.

806 Szostek, C.L., Murray, L.G., Bell, E., & Kaiser, M. J. (2017). Filling the gap: Using  
807 fishers' knowledge to map the extent and intensity of fishing activity. *Marine*  
808 *Environmental Research*, 129, 329-346.

809 The R Project for Statistical Computing. <https://www.r-project.org>.

810 Tian, Y., Wang, X., Chen, W., Liu, Z., & Li, L. (2019). Adaptive multiple classifiers  
811 fusion for inertial sensor based human activity recognition. *Cluster Computing*, 22(4),  
812 8141-8154.

813 Vapnik, V.N. (1995). The Nature of Statistical Learning Theory. *Springer New York*.